Bulletin of Geosciences, Vol. 80, No. 4, 321–354, 2005

Cenomanian and Cenomanian-Turonian boundary in the southern part of the Bohemian Cretaceous Basin, Czech Republic

Stanislav Čech [1] – Lenka Hradecká [1] – Marcela Svobodová [2] – Lilian Švábenická [1]

[1] Czech Geological Survey, Klárov 131/3, CZ-118 21 Praha 1, Czech Republic. E-mail: cech@cgu.cz, hradecka@cgu.cz, svab@cgu.cz
[2] Academy of Sciences of the Czech Republic, Institute of Geology, Rozvojová 135, CZ-165 02 Praha 6, Czech Republic.
E-mail: msvobodova@gli.cas.cz

Abstract. Initial transgressive Cretaceous deposits are described from boreholes in the southern part of the Bohemian Cretaceous Basin, i.e. siliciclastic sediments of Cenomanian age (Peruc-Korycany Formation), and hemipelagic marlstones and limestones of the Turonian age (Bílá Hora Formation). Transgressive successions include fluvial, supratidal marsh, estuarine tidal flat and channel, estuarine and mouth sand, inner shelf and open marine facies assemblages interpreted on the basis of sedimentological and paleontological features. Fluvial-estuarine facies filled an incised valley that formed a tributary of the main paleovalley in the central part of the basin. Fluvial facies are characterized by either the prevalence of spores and the presence of freshwater green algae (swampy conditions), or the prevalence of angiosperm pollen grains (alluvial plain assemblage). Marsh and estuarine facies are characterized by the presence of marine microplankton tolerant to changing salinity conditions, acritarchs, prasinophycean algae, agglutinated foraminifers, thick-walled spores, and halophyte and taxodiaceous pollen. Inner shelf facies exhibit rare sporomorphs (often thick-walled), increase of gonyaulacean dinocyst, marine macrofauna, foraminifers with non-keeled planktonic foraminifera, and sparse calcareous nannofossils. Open shelf facies are characterized by hemipelagic sediments containing keeled planktonic foraminifers and diverse calcareous nannofossils. Concerning calcareous nannofossils, the base of the Turonian is marked by the first occurrence of *Eprolithus octopetalus* (within foraminiferal *Whiteinella archaeocretacea* Interval and Partial range Zone) just above prominent erosion surface at the base of the Bílá Hora Formation. The first appearance of nannofossil species *Eprolithus moratus* coincides with first occurrence of foraminiferal planktonic species *Helvetoglobotruncana helvetica* in hemipelagic sediments of the Bílá Hora Formation.

Key words: Bohemian Cretaceous Basin, Cenomanian, Cenomanin-Turonian boundary, lithostratigraphy, depositional environment, biostratigraphy, macrofauna, foraminifers, calcareous nannofossils, palynomorphs

Introduction

In the second half of the year 2000 and in the beginning of the following year, the Aquaprotec Company Ltd. drilled hydrogeological boreholes in the south-central part of the Bohemian Cretaceous Basin (BCB) (Fig.1). The boreholes were drilled with the aim of intensifying the sources of mineral water from Cenomanian deposits in the area between Nymburk and Poděbrady-Spa.

The lithology and micropaleontology of the Cretaceous sediments in these drill cores were studied in detail by the Czech Geological Survey (CGS) and the Institute of Geology, Academy of Sciences of the Czech Republic (IGAS).

Previous studies

Although the Cenomanian sediments have been known from boreholes ever since mineral water was discovered in 1909 in Poděbrady, there is little known about the sedimentology and biostratigraphy of the Cenomanian in this area (south-central part of the BCB).

Lithological and paleontological characteristics of the Cenomanian and Turonian sediments were introduced by Klein (1966) from the west-central part of the BCB, and by Klein et al. (1982) from the east-central part of the BCB. Some problems concerning the sedimentology, sequence stratigraphy, biostratigraphy, and geochemical anomalies at the Cenomanian-Turonian (Ce-Tu) boundary have been investigated in the west-central part of the Bohemian Cretaceous Basin by Uličný et al. (1993, 1997a, b). In the Poděbrady area, the lithology, paleogeography, and tectonics of the Cenomanian and Turonian sediments were studied from boreholes by Hruška et al. (1968), and more recently by Čech (2004).

Biostratigraphically, Upper Cenomanian macrofauna was characterized by Pražák in his unpublished report (1989) from the central part of the BCB, and by Svoboda (1998) from the SW margin of the BCB. Macrofaunal assemblages and the characteristics of the microfauna and microflora of rocky shore sediments from the southern margin of the BCB have been described by Eliášová (1997), Svobodová (1990), Štemproková-Jírová (1991), and Žítt et al. (1997a, b).

In the study area, Hercogová (1968) was the first to record early Turonian foraminifers in the cores of some boreholes (OP-4 Vrbice, OP-5 Velké Zboží, OP-6 Choťánky). Macrofauna, foraminiferal assemblages, and calcareous nannofossils from the Cenomanian-Turonian boundary interval have been described in this region from the borehole Kouty BJ-16 (Hradecká et al. 1997).

Calcareous nannofossils from the Cenomanian-Turonian boundary interval have already been studied in some localities and boreholes in the BCB, unfortunately without any success (Hradecká and Švábenická 1995). Cenomanian deposits were usually barren of this fossil group, whereas the lowermost Turonian sediments contained rich assemblages. Poor coccolith assemblages in Cenomanian

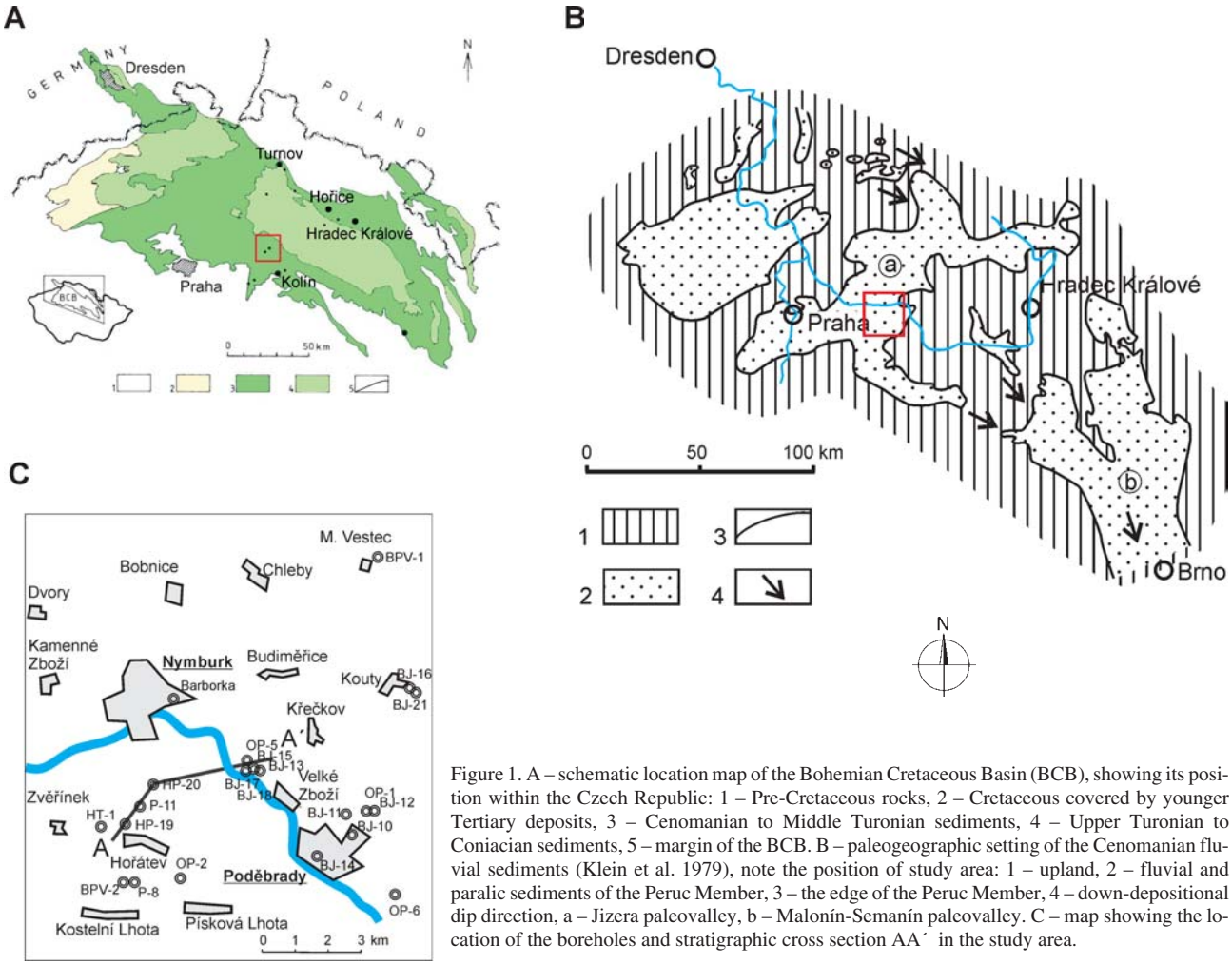

Figure 1. A – schematic location map of the Bohemian Cretaceous Basin (BCB), showing its position within the Czech Republic: 1 – Pre-Cretaceous rocks, 2 – Cretaceous covered by younger Tertiary deposits, 3 – Cenomanian to Middle Turonian sediments, 4 – Upper Turonian to Coniacian sediments, 5 – margin of the BCB. B – paleogeographic setting of the Cenomanian fluvial sediments (Klein et al. 1979), note the position of study area: 1 – upland, 2 – fluvial and paralic sediments of the Peruc Member, 3 – the edge of the Peruc Member, 4 – down-depositional dip direction, a – Jizera paleovalley, b – Malonín-Semanín paleovalley. C – map showing the location of the boreholes and stratigraphic cross section AA´ in the study area.

strata were recorded only in some boreholes situated in the central part of basin (Švábenická 2004). This study is the first to present data on calcareous nannofossils from the Cenomanian-Turonian interval of this area.

Middle–Late Cenomanian palynofacies (freshwater, transitional, and marine) and palynological assemblages from the west-central part of the BCB were studied by Pacltová and Svobodová (1993), Uličný et al. (1997 a, b), Svobodová et al. (1998), Méon et al. (2004).

Geological setting

The Bohemian Cretaceous Basin (Cenomanian-Santonian) is an intra-continental basin formed during the mid-Cretaceous as a seaway between the North Sea Basin and the Tethys Ocean. The BCB was formed by the reactivation of a fault system in the Variscan basement of the Bohemian Massif during the mid-Cretaceous (Uličný 1997, 2001).

Individual sub-basins and adjacent source areas (West and East Sudetic Islands, Central European Island) were separated by WNW to NW-trending, principal displacement fault zones (Uličný 1997). These fault zones, together with subordinate NW and NNE-directed fault zones, significantly influenced the basin topography and the basin filling in the initial stage of a marine transgression during the Cenomanian. The marine transgression created a fluvial-estuarine depositional setting with a system of paleovalleys separated by topographical highs. Two principal paleovalleys were recognized based on subsurface data: the SE trending Semanín-Malonín paleovalley in the SE part of the BCB directed to the Tethys ocean (Frejková and Vajdík 1974), and the NNE-oriented paleovalley in the central part of the basin (Klein et al. 1979, Uličný et al. 2003) (Fig. 1B).

In the study area, the Cenomanian fluvial-estuarine deposits represent the southern (landward) part of the paleodrainage system of the central paleovalley (Uličný et al. 2003, Čech 2004). New hydrogeological and balneological boreholes have penetrated the Upper Cretaceous sediments of the Bílá Hora (Lower-Middle Turonian) and Peruc-Korycany (Cenomanian) formations sensu Čech et al. (1980).

Material and methods

For correlation purposes, and for sedimentological and paleogeographical interpretations, older and recent balneological and hydrogeological boreholes, as well as some from the uranium industry, were studied (Fig. 1C). The division of Cenomanian strata into several facies associations was made on the basis of a detailed description of lithology, and the re-

cognition of major bounding surfaces in the cores together with characteristic faunal, floral, and biogenic contents, as was done in the Pecínov Quarry in the SW part of the BCB (Uličný et al. 1997a). Several stratigraphic cross sections were constructed across the area to provide a correlation framework. Lithostratigraphic subdivision of the Cretaceous deposits in the cores was used according to Čech et al. (1980). Regional genetic-stratigraphic units (CEN 1–6) based on the correlation of well-logs (Uličný et al. 2003) is still in progress and cannot be used in this paper.

Cores for litho- and biostratigraphic studies were obtained from boreholes Velké Zboží BJ-17 (83.0–110.4 m), BJ-18 (83.0–121.85 m), Hořátev HP-19 (76.0–148.6 m), Nymburk HP-20 (81.0–155.5 m), and Velké Zboží OP-5 (80.0–123.6 m) (Fig. 1C).

Samples for the study of foraminifers, calcareous nannofossils, and palynomorphs were disintegrated in the CGS Laboratory in Prague using standard methods. Macrofauna, foraminifers, and smear slides with nannofossils are housed in the CGS.

Foraminifers were separated under binocular microscope, and photographs of species were taken using scanning electron microscope. Planktonic zonation by Robaszynski and Caron (1995) was used for the correlation of the studied samples. Foraminiferal assemblages were compared with others of the same age from older material archived at CGS from the 1960s and 1970s.

Nannofossils and foraminifers were studied from the same samples. Suspension slides were prepared using a decantation method, separated fraction 3–30 μm. Slides were inspected with a Nikon light-microscope at 1000x magnification. Quantitative data are based on cca 300–500 specimens. Biostratigraphic data were correlated with the standard nannoplankton zones (CC) of Sissingh (1977), and with the Upper Cretaceous (UC) nannofossil zones of Burnett (1998).

Palynomorphs were studied only from the Cenomanian part of the boreholes. Palynological processing followed standard procedures involving HCl-HF-KOH, acetolysis, and HNO_3. Slides were examined on Zeiss-Amplival and OPTON light-microscopes. Quantitative analysis is based on 200 specimens. The slides and residues used in this study have been deposited in the Laboratory of Paleobiology and Paleoecology of the IGAS.

Results

Lithostratigraphy

Peruc-Korycany Formation

Based on the core samples, the Peruc-Korycany Formation can be subdivided into three members: the Peruc, Korycany (Čech et al. 1980), and Pecínov (Uličný 1992) members (Figs 2 and 3).

The lower part of the Peruc Member consists of fining-upward cycles of grey sandstones and conglomerates with interbeded light and dark grey mudstones. The upper part of the member also contains grey sandstones and conglomerates, but the mudstones dominate this section and have associated root zones. Carbonaceous plant debris is common. Fossil leaves are less common. In borehole HP-19, the sand-dominated, upward-coarsening cycles occur in the upper part of the Peruc Member. Driftwood fragments penetrated with borings of marine bivalves are sparsely distributed in this sandstone. In the uppermost part of the member, finely laminated black mudstones with lenses and interbeds of glauconitic siltstones and fine-grained sandstones are developed. Sand-filled burrows are conspicuous in this facies: *Thalassinoides, Planolites*, and *Teichichnus* are dominant. Thin layers of coarse-grained sandstones appear in the heterolithic beds.

The Korycany Member consists of well-sorted fine and medium grained quartzose sandstones and clayey sandstones. Sandstones locally contain a high amount of glauconite. Well-sorted sandstones contain thin layers of plant material and mud drapes, usually within cross-bed sets. Discrete sand-filled burrows of *Thalassinoides*, *Ophiomorpha*, *Diplocraterion*, and the absence of primary sedimentary lamination, indicate extensive bioturbation. In the middle and upper part of the Korycany Member, a thin heterolithic facies was observed in the core. The facies include interbedded sandstone and mudstone as sand streaks in mud, that pass into lenticular, wavy, and flaser bedded sandstone. The sediments are densely bioturbated. In some cores (HP-19, BJ-17), a thin pebbly bed (up to 0.1 m in thickness) with an erosive base was observed in the middle part of the Korycany Member.

The Pecínov Member (Uličný 1992) is characterized by dark grey, clayey, variably calcareous, very fine glauconitic siltstones that contain brown phosphatic nodules, pyrite, sponge spicules, numerous *Chondrites* burrows, and marine macrofauna in which bivalves dominate. A thin bed of glauconitic pebbly sandstone is developed at the base of the Pecínov Member. This bed is associated with a prominent erosional surface at its base.

Bílá Hora Formation

The Bílá Hora Formation is comprised of dark grey to grey marlstones and micritic limestones (Figs 2 and 3). At the base of the formation, a thin, very glauconitic, green, sandy marlstone bed is developed, associated with an erosive surface at the base of the bed (Fig. 15). This glauconitic marlstone bed contains dark brown phosphatic nodules, quartz pebbles, and dense *Chondrites* burrows. *Thallassinoides* burrows pipe glauconitic sediment down into the underlying siltstones of the Pecínov Member.

Macrofauna

A sparse marine macrofauna was recognized in the clayey siltstones of the lower part of the Pecínov Member (Figs 2 and 3). Broken shells of the bivalve *Perna cretacea* are common in the cores of HP-19 (113.1–113.95 m), HP-20 (116.55–117.0 m), and BJ-18 (107.1 m). Occasionally, the

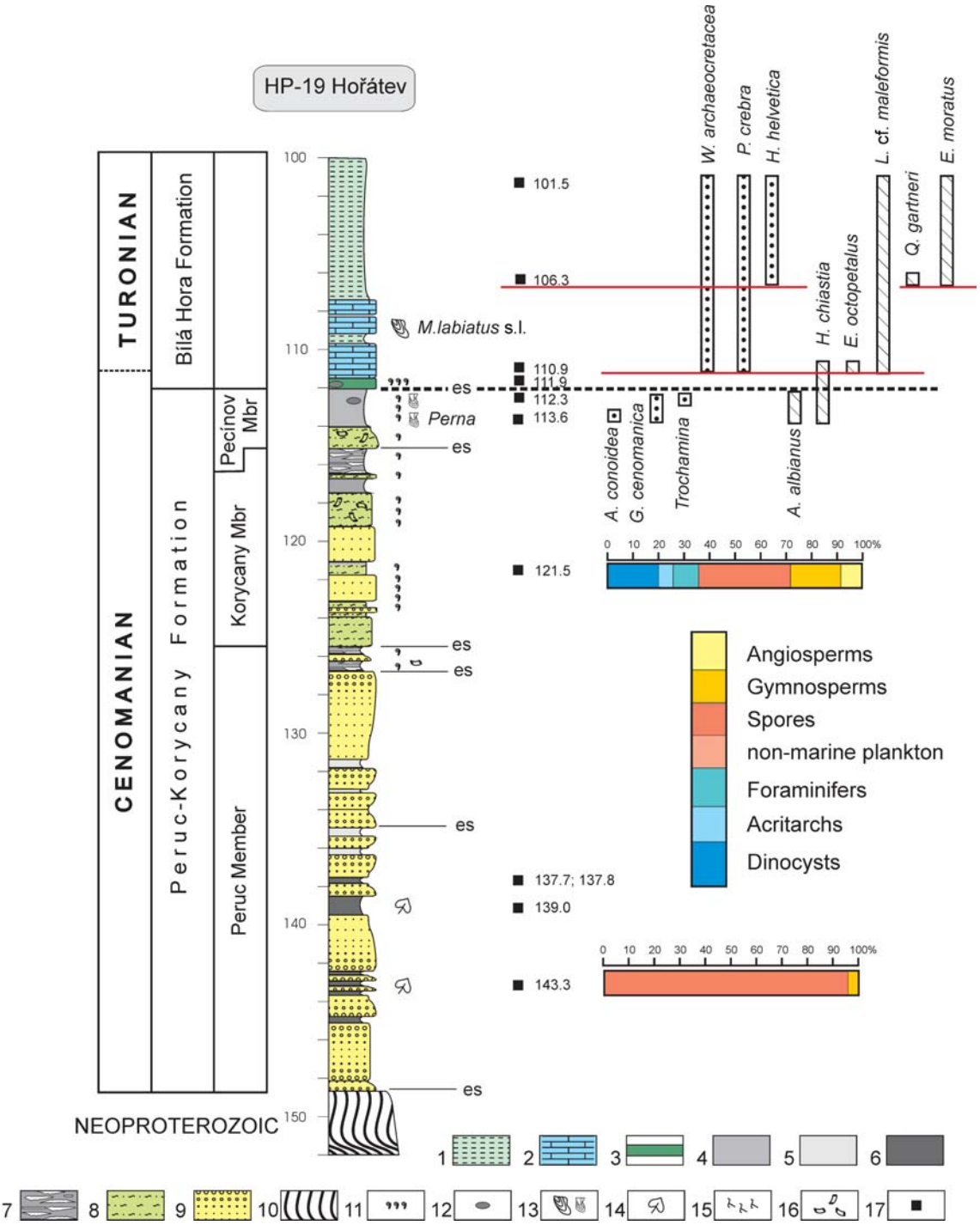

Figure 2. Lithology and distribution of macrofauna, foraminifers, calcareous nannofossils, and palynomorphs in the borehole Hořátev HP-19.
1 – marlstones, 2 – micritic limestones, 3 – glauconitic bed, 4 – calcareous clayey siltstones, 5 – claystones, 6 – carbonaceous claystones, 7 – alternation of sandstones and claystones, 8 – clayey sandstones, 9 – quartzose sandstones, 10 - metamorphosed rocks, 11 – glauconite, 12 – phosphatic nodules, 13 – macrofossils, 14 – plant macrofossils, 15 – plant roots, 16 – bioturbations, 17 – sample for micropaleontology analysis, es – erosion surface.

bivalve *Nuculana* sp. was recognized in the lower part of the Pecínov Member in borehole HP-20 (117.0 m), while the pectinid bivalve *Syncyclonema* sp. was found in borehole OP-5 (104.5 m), and *Chlamys robinaldina* in borehole BJ-18 (107.15 m).

The glauconitic bed at the base of the Bílá Hora Formation contains only small oysters. In the lower part of the Bílá Hora Formation, only fragments of the inoceramid bivalve *Mytiloides* sp. were observed in marlstones 3 m above the base of the Bílá Hora Formation in borehole HP-19 (108.9 and 105.7 m). Higher in the section, *Mytiloides* cf. *subhercynicus* appears approximately 17–19 m above the base of the Bílá Hora Formation in boreholes BJ-17 (86.5 m) and BJ-18 (87.8 m).

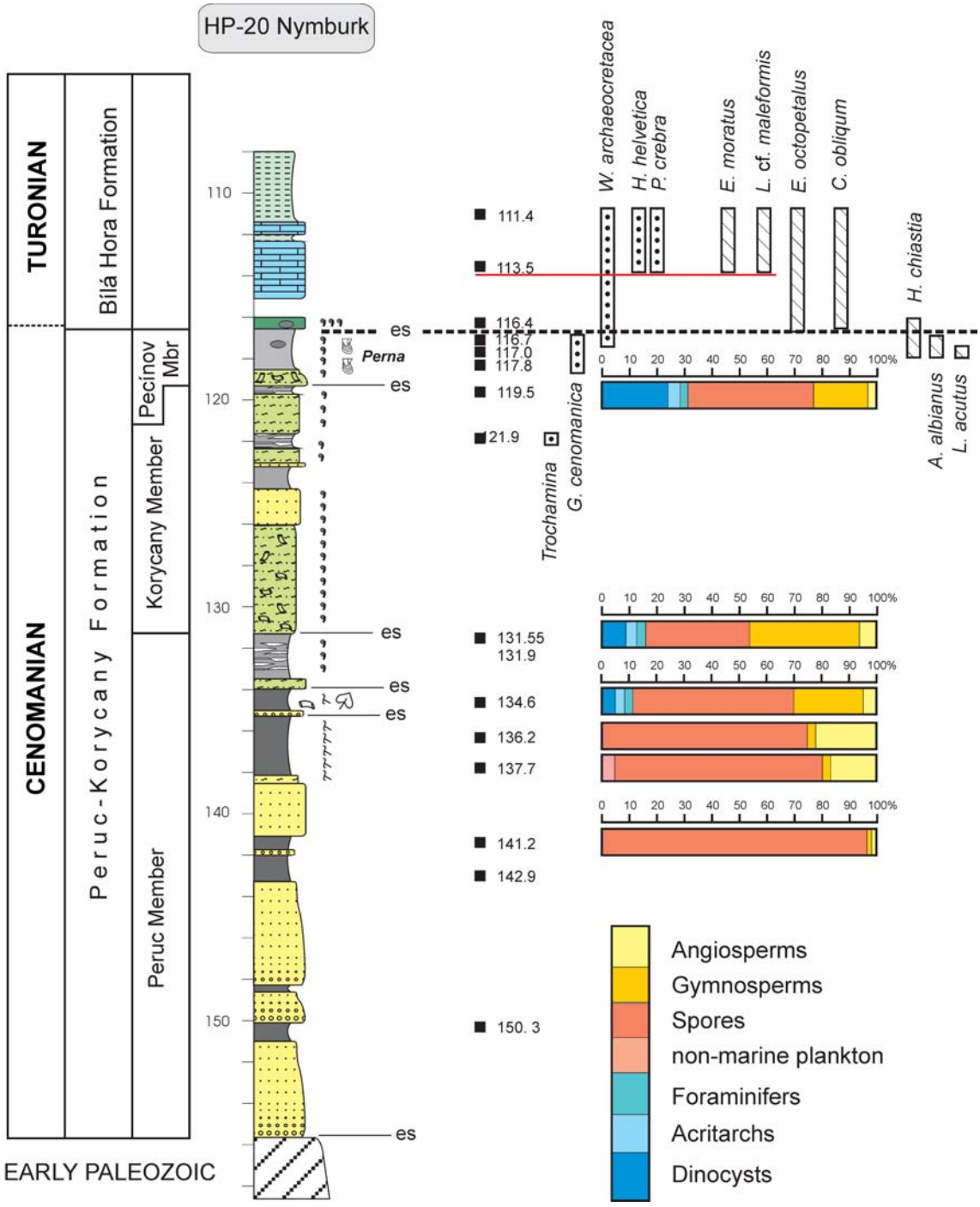

Figure 3. Lithology and distribution of macrofauna, foraminifers, calcareous nannofossils and palynomorphs in the borehole Nymburk HP-20.

Foraminifers

In borehole HP-19, *Gavelinella cenomanica* appears together with *Valvulineria lenticula* and *Ataxophragmium depressum* in siltstones of the Pecínov Member, 0.3–1.4 m below the base of glauconitic bed of the Bílá Hora Formation (Figs 2 and 4). In this stratigraphic level agglutinated species of *Arenobulimina, Haplophragmoides, Ammobaculites, Trochammina, Bigenerina*, and *Pseudotextulariella* are common. Minor components of these assemblages are calcareous forms represented mainly by *Gavelinella schloenbachi* and *Planularia complanata*. Moreover, planktonic species are again very rare. Only *Hedbergella delrioensis* and *Whiteinella brittonensis* were sporadically found.

The washed material from the lowermost Upper Cenomanian sample from borehole HP-20 (121.9 m) contained rare agglutinated species such as *Dorothia filiformis*, *Ammobaculoides lepidus*, and more frequently *Trochammina obliqua*. Only three specimens of *Gavelinella cenomanica* were found with decalcified and damaged tests. In general, agglutinated species of the genera *Arenobulimina, Haplophragmoides, Ammobaculites, Trochammina, Bigenerina*, and *Pseudotextulariella* were

abundant in the studied samples of this stratigraphic level (HP-19 113.6–112.3 m, HP-20 117.0–116.7 m, BJ-16 178.1–177.9 m, BJ-18 107.3 m). *Gavelinella schloenbachi* and *Planularia complanata* were rare here. From plankton only *Hedbergella delrioensis* and *Whiteinella brittonensis* were sporadically found (Fig. 5).

In the lower part of the glauconitic bed, at the base of the Bílá Hora Formation, inorganic material (glauconite and pyrite) prevailed in boreholes HP-19 (111.9 m) and HP-20 (116.4 m) (Figs 4–7). The foraminiferal assemblage is generally poor: only agglutinated *Arenobulimina preslii* and a few specimens of the calcareous *Lingulogavelinella* and *Gavelinella* were found.

Diversity of the foraminiferal assemblages increases gradually in the overlying sediments, i.e. in the upper part of the glauconitic bed (in boreholes BJ-17 from 103.2 m, BJ-18 from 106.5 m, and BJ-16 from 177.3 m) and the micritic limestones (in boreholes HP-19 from 110.9 m, and HP-20 from 113.5 m). The foraminiferal assemblage is characterized by the frequent occurrence of *Praebulimina crebra*, *Gavelinella polessica*, *G. belorussica, G. berthelini, Cassidella tegulata*, and *Valvulineria lenticula.* Planktonic foraminifera are represented by *Hedbergella, Whiteinella*, and *Heterohelix.* Some specimens of *Helvetoglobotruncana helvetica* were found in the micritic limestones and marlstones, approximately 3–8 m above the base of the Bílá Hora Formation. Foraminifera with agglutinated tests are represented by the genera *Gaudryina, Gyroidina*, and *Dorothia* (Figs 4 and 5).

Calcareous nannofossils

Calcareous nannofossils were found exclusively in the grey calcareous siltstone of the Pecínov Member (in boreholes Hořátev HP-19 (113.6–111.9 m), and Nymburk HP-20 (117.8–116.7 m) (Figs 8 and 9). These deposits contain low- to mid-abundance assemblages (10–20 specimens per 1 field of view of microscope) with medium-well or poorly preserved nannofossils. Coccoliths are etched, mostly in fragments, and the central areas of placoliths are usually dissolved. The assemblages contain the marker species *Axopodorhabdus albianus* (Plate III, figs 16–18) and *Helenea chiastia*, and relatively high numbers of *Watznaueria barnesae* (35–40 %, Plate IV, fig. 17), *Prediscosphaera columnata* (6–7 %), and *Broinsonia signata* (10–12 %). A characteristic phenomenon is the presence of large, broadly elliptical specimens of *Manivitella pemmatoidea* (see Plate IV, figs 31, 32).

Calcareous nannofossils from the Pecínov Member occur in the Nymburk HP-20 borehole at a depth of 117.8 m, representing only a small number of specimens of long-ranging taxa. The quantity and species diversity quickly increases in the overlying strata (see Fig. 11). The scarce presence of the stratigraphically significant *Lithraphidites acutus* (Plate IV, figs 33, 34) and *Corollithion kennedyi* (see Plate IV, figs 1, 2) was recorded from the Nymburk HP-20 borehole exclusively, at a depth of 117.0 m (see Plate 3, figs 1, 2 and 33, 34). The relatively common occurrence of *A. albianus*, and its sudden disappearance, were observed in both boreholes.

The character of the nannofossil associations is markedly different in the green glauconitic sandy marlstones (Bílá Hora Formation) of boreholes Velké Zboží BJ-17, BJ-18, Hořátev HP-19, and Nymburk HP-20 (Figs 8–11). High-abundance assemblages (40–50 specimens per field of view under the microscope) are typical for these strata. Nannofossils are well or medium-well preserved and remarkably small in size, especially in the lowermost part of the sequence. The deposits contained *Eprolithus octopetalus* (Plate III, figs 29, 30), *Ahmuellerella octoradiata,* and *Quadrum intermedium* (5 and 7 ray-like elements) among others. *Helenea chiastia* was recorded only in the lowermost part of these strata. Specimens of the genus *Broinsonia* becomes rare (*B. signata* 1 %, *B. enormis* 4 % in maximum). High content of *Watznaueria barnesae* varies between 43–47 %, and this percentage slightly decreases up to 35 % in the overlying beds. The size of nannofossils quickly returns to the standard norm. The character of nannofossil assemblages also remains very similar in the lower part of the overlying micritic limestones with an admixture of glauconite.

Up-section, the first occurrences of *Eprolithus moratus* (Plate III, figs 31, 32) and *Lucianorhabdus* cf. *maleformis* (Plate IV, figs 28–30) are observed, whereas *Eprolithus octopetalus* disappears (Figs 2 and 3). The assemblages contain higher numbers of the "subtle" specimens of the family Stephanolithiaceae, such as *Corollithion signum, C. exiguum, Cylindralithus biarcus*, and *Rotelapillus crenulatus*. Calcareous nannofossils were not studied from the deposits of borehole Velké Zboží OP-5.

Palynomorphs

The lower part of borehole Hořátev HP-19 (depth 143.3 m) is characterized by a well-preserved palynomorph assemblage consisting predominantly of fern spores (94 %) of Schizaeaceae and Gleicheniaceae. Gymnosperm pollen grains rarely occur (Figs 12, 13). Samples from the depth interval 137.7–139.0 m were barren. Marine microplankton (40 %) appear in the upper part of the HP-19 borehole (121.5 m). The terrestrial content includes bryophyte and pteridophyte spores (35 %), gymnosperm pollen (20 %), and angiosperm pollen grains (5 %). Pteridophyte spores consist of the Gleicheniaceae, Lycopodiaceae, and Cyatheaceae. *Classopollis classoides* and *Taxodiaceaepollenites hiatus* prevail among the gymnosperm pollen. *Classopollis/Corollina* pollen is often found in tetrads, suggesting a negligible distance of transport. The dinocyst assemblage includes littoral forms such as *Circulodinium distinctum* and *Epelidosphaeridia spinosa*, or neritic types such as *Spiniferites ramosus.*

In the mudstones of the lower part of borehole HP-20 Nymburk, a poor palynomorph assemblage of predominantly freshwater origin was found at 150.3 m, associated with a small percentage of acritarchs and halophyte pollen. A sample from 141.2 m contains an assemblage with a high percentage of angiosperms (42 %). A similar assemblage was recorded in the mudstone of Unit 1 of the Pecínov quarry (Uličný et al. 1997a, Svobodová et al. 1998). Two

HOŘÁTEV HP-19	Upper Cenomanian		Lower Turonian			
	Whiteinella archaeocretacea Zone				*Helvetoglobotruncana helvetica* Zone	
depth (m)	113.6	112.3	111.9	110.9	106.3	101.5
Gyroidina nitida					○	●
Hagenowina advena	x					
Arenobulimina preslii	x		x			
Ataxophragmium depressum	x	○				
Bigenerina selseyensis	x					
Haplophragmoides nonioninoides		x				
Trochammina obliqua		x				
Ammobaculites reophacoides		x				
Pseudotextulariella cretosa		x				
Dorothia gradata		x				
Haplophragmoides stelcki		x				
Trochammina globosa		x				
Gaudryina praepyramidata					○	
Dorothia filiformis					x	x
Gaudryina variabilis					x	
Praebulimina crebra				●	●	●
Lenticulina sp.	x		x		x	○
Gavelinella cenomanica	○	○				
Gavelinella schloenbachi	x			x		
Nodosaria obscura		x				
Valvulineria lenticula		○		○	●	●
Marginulina robusta		x				
Nodosaria bistegia		x				
Lingulogavelinella globosa			○	x		x
Gavelinella belorussica			○	x		
Gavelinella polessica				○	○	●
Cassidella tegulata				x	x	
Gavelinella berthelini			○	x		x
Frondicularia verneuiliana					x	
Ramulina globulifera						x
Vaginulina robusta						x
Lenticulina comptoni						x
Frondicularia inversa						x
Gavelinella baltica			x			x
Lingulogavelinella pazdroae						x
Whiteinella archaeocretacea				○	x	x
Hedbergella delrioensis	x			○	○	○
Whiteinella brittonensis			x	x	○	x
Whiteinella aprica			x	x		
Heterohelix pulchra				○	○	●
Helvetoglobotruncana helvetica					x	x
Praeglobotruncana delrioensis					x	x
Hedbergella simplex			x			
Hedbergella planispira					x	
Whiteinella baltica					○	
Dicarinella imbricata					x	

Figure 4. Distribution of foraminiferal species in Hořátev HP-19 borehole.
● abundant, ○ common, x rare, ? questionable

NYMBURK HP-20	Upper Cenomanian			Lower Turonian			
	Whiteinella archaeocretacea Zone					*H. helvetica* Zone	
depth (m)	121.9	117.8	117.0	116.7	116.4	113.5	111.4
Gaudryina praepyramidata						x	x
Gaudryina angustata							x
Dorothia filiformis	x					x	x
Gyroidina nitida							○
Gaudryina folium							x
Dorothia gradata				x			x
Gaudryina trochus						x	x
Textularia foeda							x
Trochammina obliqua	○						x
Marssonella oxycona						x	
Dorothia turris						x ?	
Haplophragmoides sp.			x	x			
Haplophragmoides ovalis				○			
Ammobaculites reophacoides				x			
Ataxophragmium depressum			○	x			
Ammodiscus gaultinus				x			
Spiroplectammina scotti		x					
Lituotuba incerta		x					
Ammobaculoides lepidus	○						●
Cassidella tegulata						x	
Praebulimina crebra						●	○
Dentalina sp.				x		x	x
Valvulineria lenticula					x	●	●
Lenticulina sp.				x		x	x
Ramulina globulifera						x	x
Vaginulina robusta							x
Gavelinella polessica						○	○
Frondicularia verneuiliana							x
Lenticulina comptoni				x		○	○
Frondicularia sp.						x	x
Planularia complanata			x	x			x
Nodosaria obscura							x
Gavelinella belorussica					x	x	
Gavelinella berthelini						○	
Lingulogavelinella globosa					○	x	
Gavelinella cenomanica	x ?	○	○	●			
Marginulina aequivoca				x			
Gavelinella schloenbachi		x					
Whiteinella brittonensis		x			○	○	●
Hedbergella delrioensis						○	●
Heterohelix globulosa							○
Whiteinella paradubia						x	○
Whiteinella archaeocretacea				x	x		x
Hedbergella planispira						x	x
Helvetoglobotrun. praehelvetica					x	x	○
Helvetoglobotruncana helvetica						x	x
Whiteinella aprica					x		x
Heterohelix pulchra						x	
Dicarinella imbricata							x
Whiteinella baltica						x	

Figure 5. Distribution of foraminiferal species in Nymburk HP-20 borehole. For explanations see Fig. 4

VELKÉ ZBOŽÍ BJ-17	Upper Cenomanian		Lower Turonian							
	W. archaeocretacea Zone		*Helvetoglobotruncana helvetica* Zone							
depth (m)	105.1	103.5	103.2	102.3	100.8	95. 1	90. 1	85. 0–85. 1	82. 0–82. 5	50.5
Gaudryina folium								x		x
Ataxophragmium depressum		x							x	x
Vaginulina robusta					x		x			x
Frondicularia verneuiliana				x	x	x				x
Gavelinella berthelini			x	x	○	●	○		○	○
Frondicularia fritschi										x
Frondicularia inversa						x				x
Gavelinella polessica			x		x	○	○	x		●
Gaudryina variabilis									x	x
Praebulimina crebra			x	x	x	x	●	○	○	●
Cassidella tegulata				x		○	●	●	x	○
Textularia foeda							x			x
Spiroplectammina sp.	x									
Gaudryina angustata				x				x	x	x
Arenobulimina preslii			x	x		○		x		○
Gaudryina praepyramidata						x		x	x	x
Vaginulina recta										x
Gaudryina trochus								x		x
Gavelinella belorussica			x	x	●	○				○
Lingulogavelinella pazdroae										x
Valvulineria lenticula			x	x	○	○	○	x	x	●
Gavelinella schloenbachi			x	x	x	○		x		x
Lingulogavelinella globosa			x	x			○			○
Gavelinella baltica			x	x				x		
Pseudotextularia cretosa	x									
Haplophragmoides sp.	x									
Whiteinella paradubia					x	x				x
Whiteinella brittonensis		x	x	x	○	x	x	x	x	○
Hedbergella planispira										x
Dicarinella imbricata			x					x		x
Helvetoglobotruncana helvetica						x		x	x	x
Heterohelix globulosa			x		○				x	○
Helvetoglobotruncana praehelvetica				x			○			x
Whiteinella archaeocretacea				x						
Heterohelix pulchra					x		x			
Praeglobotruncana delrioensis				x						
Ramulina globulifera						x			x	
Tappanina eouvigeriniformis			x	x						
Lenticulina sp.				x	x	x	x	x	x	x
Trochammina sp.	x								x	x
Dorothia turris					x	x				x
Quadrimorphina allomorphinoides								x	x	
Ammobaculites reophacoides										x
Hagenowina advena		x								
Dorothia oxycona								x	x	

Figure 6. Distribution of foraminiferal species in Velké Zboží BJ-17 borehole. For explanations see Fig. 4.

VELKÉ ZBOŽÍ BJ-18	Upper Cenomanian				Lower Turonian							
	Whiteinella archaeocretacea Zone							*Helvetoglobotruncana helvetica* Zone				
depth (m)	113.3–113.4	112.5	108.4	107.3	106.5	106.3	105.5	102.4	98.3–98.4	93.9–94.0	88.0–88.1	83.0–83.1
Gavelinella berthelini				x				x	○		x	○
Gyroidina nitida										x	x	○
Ataxophragmium depressum				x								x
Cassidella tegulata									x	○	○	x
Arenobulimina preslii				x						x	○	○
Nodosaria sp.												x
Lingulogavelinella globosa				x	x	○	●	●	○			x
Lenticulina sp.					x	x		x	x	x	x	x
Gaudryina folium												x
Gavelinella schloenbachi												x
Whiteinella brittonensis							x	○	○	x	x	x
Helvetoglobotrunc. helvetica								x	x		x	x
Vaginulina robusta							x	x	x		x	x
Gaudryina angustata										x	x	x
Gavelinella polessica							○		x			●
Dicarinella imbricata						x	x	○		x		x
Whiteinella paradubia						x	x	x		x	x	x
Frondicularia verneuilina						x					x	x
Frondicularia inversa							x	x		x		x
Lingulogavelinella pazdroae									x		x	x
Trochammina obliqua	x	x		x								x
Whiteinella baltica						x		○		x	x	x
Gavelinella baltica									x		x	x
Lenticulina comptoni						x	x		x			x
Frondicularia fritschi						x					x	x
Valvulineria lenticula						x	○	○		x		●
Hedbergella delrioensis					x			●		x		x
Ramulina globulifera						x						x
Gaudryina praepyramidata					x	x	x		x	x	x	
Gavelinella belorussica	x				x	○	x		x		x	
Textularia foeda										x	x	
Gaudryina trochus										x	x	
Gaudryina compressa ?										x	x	
Hedbergella planispira					x	x		x		x		
Marssonella oxycona				x				x		x		
Whiteinella aprica						x				x		
Praeglobotruncana oraviensis							x	x		x		
Helvetoglob. praehelvetica						○	x	○	○	x		
Praeglobotruncana delrioensis						x		x	x	x		
Dorothia filiformis				x		x	x	x	x			
Dorothia turris									x			
Whiteinella archaeocretacea				x				x	x			
Gavelinella cenomanica				x								
Ammodiscus cretaceus				x				x				
Vaginulina recta						x						
Haplophragmoides sp.				x								

Figure 7. Distribution of foraminiferal species in Velké Zboží BJ-18 borehole. For explanations see Fig. 4.

new types of angiosperm pollen appear: tetracolpate form aff. *Stephanocolpites*, and very small foveolate pollen aff. *Foveotetradites fistulosus* configured in tetrads (see Pl. VI). Non-marine sedimentation continues to the depth of 137.7 m (dark sandy mudstone), the percentage of pteridophyte spores increases while the amount of angiosperm pollen decreases. The diversification of angiosperm pollen remains high, among which the periporate species *Bohemiperiporis zaklinskae* appears. The first true marine influence occurs at a depth of 134.6 m (Peruc Member). Dinocysts (8 %) consist mainly of *Palaeohystrichophora infusorioides, Circulodinium, Cleistosphaeridium*, and *Spiniferites.* Chitinous foraminiferal linings (3 %) are also present. Pteridophyte spores prevail. Gymnosperm pollens are represented mainly by Taxodiaceae, with less-numerous inaperturate forms such as *Cycadopites fragilis, Eucommiidites minor*, and bisaccate pollen. An isolated record of *Ephedripites jansonii* and *Araucariacites australis* occurs. Angiosperm pollen is diverse and well preserved. Freshwater green zygnematacean algae *Chomotriletes minor* and *Ovoidites parvus* were identified. A similar marine content with an increasing amount of gymnosperm pollen (40 %) was recorded in dark grey clayey siltstone laminated with glauconite sandy claystone (131.9 m). Specimens of *Classopollis/Corollina*, together with bryophyte spores and pteridophyte spores dominate in the palynospectrum. Palynomorphs from the upper part of borehole HP-20 (119.5 m) are comparable to those from HP-19 (121.5 m). Pteridophyte spores prevail (45 %). *Classopollis classoides* and *Taxodiaceaepollenites hiatus* are the most common among gymnosperm pollen. Angiosperm pollen is rare. The percentage of marine microplankton increases (27 %), but the diversity remains low. The assemblage from borehole Velké Zboží OP-5 (122.3 m) is similar to that found in HP-19 (143.3 m), and it is characterized by the dominance of pteridophyte spores (93 %). Angiosperm pollen (4 %) consists of reticulate tricolpate and tricolporate forms. Changing conditions are recorded in the OP-5 borehole (112.4 m), where the marine influence is documented by the appearance of dinocysts (16 %) such as *Odontochitina, Xenascus, Palaeohystrichophora,* and *Circulodinium.* The percentage of pteridophyte spores decreases (36 %). Gymnosperm pollen (36 %) consists mainly of Taxodiaceae and *Classopollis/Corollina* pollen. Angiosperm pollen is rare, while Cenomanian species and the triporate pollen of *Complexiopollis* appear more commonly. The terrestrial content (spores, and gymnosperm and angiosperm pollen) and non-marine algae constitutes 96 % of the assemblage, with a minor marine contribution of dinocysts (*Epelidosphaeridia, Circulodinium*), foraminifers, and prasinophycean algae in the BJ-18 borehole (121.7 m). The palynomorph assemblage is well preserved and diversified. Pteridophyte spores prevail (49 %) (Gleicheniaceae, Schizaeaceae, Matoniaceae, Polypodiaceae). Bisaccate gymnosperm pollen including *Parvisaccites radiatus* and *Alisporites bilateralis* prevail, while *Ephedripites multicostatus* and *Sequoiapollenites* sp. rarely appear.

Lithological and paleoenvironmental interpretations

Depositional environment, facies assemblages, and bounding surfaces

Six facies assemblages were recognized in the Peruc-Korycany Formation: fluvial facies, estuarine bayhead delta, supratidal marsh facies, estuarine tidal flat and channel facies, estuarine and mouth sand facies, and inner marine facies. Open shelf facies include hemipelagic marlstones and limestones of the Bílá Hora Formation (Fig. 14).

Fluvial channel deposits (conglomerates and sandstones) and overbank deposits (siltstones, siltstones with coal seams and root zones) of an alluvial plain were recognized in boreholes HP-19 and HP-20, located in the axial position of the incised-valley fill (Fig. 14), and in borehole OP-5 situated on the slope of paleoelevation. These deposits are interpreted as part of the drainage system of a main paleovalley parallel to the present Jizera River (Klein et al. 1979, Uličný et al. 2003) (Fig. 1B). According to palynomorphs, the prevalence of pteridophyte spores and taxodiaceous pollen in the mudstones suggests swampy vegetation. The high percentage of angiosperm specimens in comparison with fern spores and gymnosperms only rarely occurs. This probably represents an alluvial plain assemblage consisting of shrubby and arboreal plants (Uličný et al. 1997a).

Estuarine bayhead delta facies were recognized in borehole HP-19. These facies comprise sand dominated upward-coarsening cycles of coarse-grained sandstones, occurring where the tributary entered the estuary. The occurrence of borings of marine bivalves indicates tidal influence. First marine influence in the environment is also documented by the appearance of acritarchs, chitinous foraminiferal linings, and mostly broken specimens of ceratioid and peridinioid dinocysts. Sometimes together with the marine plankton, non-marine elements occur. This bayhead delta facies disconformably overlies fluvial facies, as well as supratidal marsh facies and estuarine tidal flat and channel facies (Fig. 14).

Supratidal marsh facies are evident in borehole HP-20 as rooted mudstones with plant debris. The palynologic assemblage contains marine microplankton (8 %), foraminifers, spores, and pollen grains of Taxodiaceae (HP-20, sample 134.6 m in Figs 3, 12 and 13).

Finely laminated, dark grey mudstones with ripple-laminated, lenticular, fine-grained sandstones, and thin layers of coarse-grained sandstones scoured into the older sediments, are interpreted as estuarine tidal flat and channel facies. These facies sharply overlie supratidal marsh or fluvial strata, where the bayhead delta facies is not present (boreholes HP-20 and OP-5). It disconformably overlies Neoproterozoic rocks at a topographic paleoelevation (boreholes BJ-17 and BJ-18) (Fig. 14) where fluvial sediments are missing. Tidal influence in the heterolithic sediments is documented by glauconite admixture and by a palynologic assemblage comprised of marine microplankton (13 %), foraminifers, spores, and gymnosperms

HOŘÁTEV HP-19	Upper Cenomanian			Lower Turonian		
Standard nannofossil zones Sissingh (1977), Perch-Nielsen (1985)	CC10a				CC10b	
Upper Cretaceous nannofossil zones Burnett (1998)	UC5a		UC5b	UC5c	UC6b	
depth (m)	113.6	112.3	111.9	110.9	106.3	101.9
relative sample abundance	L	M	H	H	H	H
nannofossil preservation	M	M	VP	VP	P	VP
Axopodorhabdus albianus	C	F				
Biscutum ellipticum	F	A	F	A	C	F
Broinsonia enormis	C	F	F	F	F	F
Broinsonia matalosa	R	R		VR		VR
Broinsonia signata	A	A	R	F		
Bukrylithus ambiguus	R	VR	R	VR		
Eiffellithus turriseiffelii	A	C	C	C	C	C
Eprolithus floralis	F	F	F	F	R	F
Eprolithus cf. *moratus*	?					
Gartnerago cf. *theta*	R	R		r		
Haqius circumradiatus	R		VR		VR	
Helenea chiastia	R	F		VR		
Lithraphidites carniolensis	R	R	R	F	F	F
Manivitella pemmatoidea	R	R	VR	R	VR	F
Microrhabdulus decoratus	R			VR	VR	
Perissocyclus fenestratus	R	R			R	R
Placozygus cf. *fibuliformis*	R	F	R	VR		R
Prediscosphaera columnata	C	F	F	F	F	F
Prediscosphaera cretacea	F	F	C	F	C	C
Prediscosphaera ponticula	F	F	R	R		F
Prediscosphaera spinosa	R	R		R	VR	
Rhagodiscus asper	R	F	VR	VR		VR
Rhagodiscus splendens	F					VR
Retacapsa crenulata	R	F	F	R	F	R
Rotelapillus crenulatus	F	F	F	F	F	F
Scapholithus sp.	R					
Sollasites sp.	R	R	?			
Tegumentum stradneri	F	F	F	R	F	R
Tranolithus gabalus	R	F	R		VR	R
Watznaueria barnesae	VA	VA	VA	VA	VA	VA
Watznaueria britannica	R					
Zeugrhabdotus bicrescenticus	F	F	F	F	F	F
Zeugrhabdotus diplogrammus	C	C	C	C	A	A
Zeugrhabdotus erectus	R					
Zeugrhabdotus noeliae	F	F	C	C	F	F
Amphizygus brooksii		R		R	R	
Cretarhabdus conicus		F	R	R	R	F
Microrhabdulus belgicus		VR		VR	VR	
Stoverius achylosus		VR	VR	R	VR	F
Rhagodiscus angustus		R	R	F	VR	
Rhagodiscus plebeius		VR	VR			
Chiastozygus litterarius			F	VR		F
Gartnerago obliquum			R	R	F	R
Grantarhabdus coronadventis			F	F		R

HOŘÁTEV HP-19	Upper Cenomanian			Lower Turonian		
Standard nannofossil zones Sissingh (1977), Perch-Nielsen (1985)	CC10a				CC10b	
Upper Cretaceous nannofossil zones Burnett (1998)	UC5a		UC5b	UC5c	UC6b	
depth (m)	113.6	112.3	111.9	110.9	106.3	101.9
Helicolithus compactus			R	F		R
Helicolithus trabeculatus			F	F	F	R
Retacapsa angustiforata			R			
Watznaueria biporta			R		F	R
Watznaueria fossacincta			VR	VR		R
Zeugrhabdotus embergeri			R	R	VR	R
Cribrosphaerella ehrenbergii				R	F	
Eprolithus octopetalus				R		
Lucianorhabdus cf. *maleformis*				VR	R	VR
Quadrum intermedium (5 elements)				VR	VR	
Ahmuellerella octoradiata					R	F
Corollithion exiguum					R	
Corollithion signum					R	
Cyclagelosphaera rotaclypeata					VR	
Eprolithus moratus					F	R
Quadrum gartneri					R	
Quadrum intermedium (7 elements)					R	

Figure 8. Calcareous nannofossil distribution in the Hořátev HP-19 borehole. Abundance of nannofossil taxa: VA – very abundant (> 30 %), A – abundant (30–10 %), C – common (9–5 %), F – few (4–1 %), R – rare (< 1 %), VR – very rare (only 1–2 specimens observed in slide), r – reworked specimens. Estimates of the abundance of nannofossils in samples: H – high (> 50 specimens per field of view under the microscope), M – moderate (50–20 specimens), L – low (< 5 specimens). Preservation of nannofossils: M – moderate (overgrowth, etching or mechanical damage is apparent but majority of specimens are easily identifiable), P – poor (etching and mechanical damage is extensive, making identification of some specimens difficult), VP – very poor (some specimens cannot be identified).

(mainly halophyte and taxodiaceous pollen) (HP-20, samples 131.9 m and 131.55 m in Figs 3, 12 and 13).

Massive sandstones of the Korycany Member, which are well sorted, partly highly bioturbated, and glauconitic, are interpreted as intertidal estuarine and intertidal to subtidal mouth sand facies. The sandstones sharply overlie estuarine heterolithic sand and mud facies both in the estuary valley fill and on the paleoelevation area (Fig. 14). No macrofossils were found in these sandstones. Sand-filled burrows of *Thalassinoides*, *Ophiomorpha*, and *Diplocraterion* are common. In the upper part of these sandstones, intercalations and thin layers of heterolithic sediments occur similar in lithology and palynologic assemblage to the estuarine tidal flat and channels facies, but with higher dinocyst content. The gradual relative deepening of the sedimentological basin is indicated by higher dinoflagellate cyst diversification and by the appearance of gonyaulacoid forms, i.e. *Callaiosphaeridium asymmetricum*, *Florentinia mantelii*, *Surculosphaeridium* ?*longifurcatum* (see HP-19, sample 121.5 m, HP-20, sample 119.5 m, OP-5, sample 112.4 m in Figs 2, 3 and 14). Agglutinated foraminifers (e.g. *Trochamina, Bigenerina, Ammobaculoides and Ataxophragmium*) scarcely appear in these heterolithic sediments in boreholes HP-20 (121.9 m), BJ-18 (112.5 m and 113.4 m), and OP-5 (112.5 m and 113.4 m).

The inner shelf facies consisting of calcareous, clayey, glauconitic siltstones of the Pecínov Member are documented by a marine macrofauna, foraminifers, and calcareous nannofossils (see Figs 2, 3). Among the foraminifers, mostly agglutinated species and calcareous benthos with sporadic representatives of the planktonic genera *Hedbergella* and *Whiteinella* were found.

A major erosive surface and a transgressive lag separates the inner shelf facies from the underlying strata. On the paleohighs, the Pecínov Member transgressively overlies Neoproterozoic and early Paleozoic rocks with oyster accumulations at the base (e.g. in borehole OP-6, for location see Fig. 1C).

A highly diverse foraminifer and calcareous nannofossil assemblage in the marlstones and micritic limestones of the Bílá Hora Formation, and the abundance of planktonic species with the keeled type of tests and juvenile tests of calcareous foraminifers such as *Heterohelix*, indicate open sea conditions in the Lower Turonian. This facies is separated from the underlying inner shelf facies by a prominent erosive surface associated with stratigraphic condensation (glauconitic bed) at the base of the Bílá Hora Formation. This glauconitic key bed can be identified in the boreholes and in outcrops across almost the entire BCB.

NYMBURK HP-20	Upper Cenomanian			Lower Turonian		
Standard nannofossil zones Sissingh (1977), Perch-Nielsen (1985)	CC10a				CC10b	
Upper Cretaceous nannofossil zones Burnett 1998	UC3d–UC4b		UC5a	UC5c	UC6b	
depth (m)	117.8	117.0	116.7	116.4	113.5	111.4
relative sample abundance	L	M	M	H	H	M
nannofossil preservation	VP	M	M	M	P	P
Broinsonia signata	R	C	C	R	R	R
Eprolithus floralis	A	F	F	F	R	R
Manivitella pemmatoidea	C	R	R	VR	R	F
Prediscosphaera columnata	R	C	F	F	F	F
Watznaueria barnesae	VA	VA	VA	VA	VA	VA
Watznaueria britannica	VR		VR		R	R
Watznaueria fossacincta	F			R		
Zeugrhabdotus diplogrammus	R	C	F	A	A	A
Zeugrhabdotus scutula	R	R	R	F	R	
Zeugrhabdotus sp. (outer rim)	R					
Amphizygus brooksii		VR	VR	R	F	R
Axopodorhabdus albianus		C	F			
Biscutum ellipticum		C	F	F	R	R
Broinsonia enormis		F	F	F	C	F
Broinsonia matalosa		VR		R	R	R
Bukrylithus ambiguus		R	R	F	R	
Chiastozygus litterarius		VR		R	F	R
Corollithion kennedyi		R				
Cribrosphaerella ehrenbergii		R		R	R	F
Eiffellithus turriseiffelii		F	C	C	C	A
Gartnerago cf. *theta*		R	VR			
Helenea chiastia		R	R	VR		
Helicolithus trabeculatus		F	R	F	F	F
Lithraphidites acutus		VR				
Lithraphidites carniolensis		R	F	F	F	F
Nannoconus elongatus		VR				
Placozygus cf. *fibuliformis*		VR	R	F		
Prediscosphaera cretacea		C	C	F	C	A
Prediscosphaera ponticula		F	F	F	F	
Retacapsa angustiforata		VR		F	R	
Retacapsa crenulata		F	F	F	F	R
Rhagodiscus angustus		R	F	F	F	R
Rhagodiscus splendens		VR	R	R	R	
Rotelapillus crenulatus		F	F	F	F	
Sollasites sp.		R	R	R	VR	
Tegumentum stradneri		R	F	R	R	F
Thoracosphaera sp.		R				
Tranolithus gabalus		VR	VR	R		R
Watznaueria biporta		VR	R	F		VR
Zeugrhabdotus bicrescenticus		R	F	R	F	F
Zeugrhabdotus noeliae		R	F	F	F	F
Zeugrhabdotus trivectis		R	F			
Cretarhabdus conicus			R	R		R
Grantarhabdus coronadventis			VR	R	R	F

NYMBURK HP-20	Upper Cenomanian			Lower Turonian		
Standard nannofossil zones Sissingh (1977), Perch-Nielsen (1985)	CC10a				CC10b	
Upper Cretaceous nannofossil zones Burnett 1998	UC3d–UC4b		UC5a	UC5c	UC6b	
depth (m)	117.8	117.0	116.7	116.4	113.5	111.4
Ahmuellerella octoradiata				R		R
Corollithion exiguum				R		
Corollithion signum				VR		
Eprolithus octopetalus				VR		VR
Gartnerago obliquum				R	F	F
Helicolithus compactus				F	R	R
Microrhabdulus decoratus				R	R	
Stoverius achylosus				R	F	
Tranolithus orionatus				R	VR	
Zeugrhabdotus embergeri				F		F
Zeugrhabdotus erectus				R		
Braarudosphaera bigelowii					VR	
Eprolithus moratus					R	F
Lucianorhabdus cf. *maleformis*					R	
Haqius circumradiatus						VR
Eiffellithus turriseiffelii-eximius						VR
Isocrystallithus compactus						r
Prediscosphaera spinosa						VR

Figure 9. Calcareous nannofossil distribution in the Nymburk HP-20 borehole. For explanations see Fig. 8.

Biostratigraphy

In borehole BJ-16 Kouty (Fig. 1C), Hradecká et al. (1997) reported *Pseudoptera anomala*, *Chlamys robinaldina*, *Rastellum carinatum*, *Apiotrigonia sulcataria*, and *Neithea notabilis* from calcareous siltstones of the Pecínov Member. A similar assemblage was recognized in the same level in boreholes BJ-17, BJ-18, HP-19, and HP-20. This bivalve assemblage is typical of the Pecínov Member (formerly known in the BCB as the *Actinocamax plenus* Zone) of the central and southwestern part of the BCB (Soukup and Vodička 1967, Pražák 1989, Svoboda 1998, Uličný et. al. 1997b). In these cases, the calcareous siltstones contain *Metoicoceras geslinianum* and *Praeactinocamax plenus*, both of which characterize the Upper Cenomanian *Metoicoceras geslinianum* Zone. The bivalve *Neithea notabilis* is a typical fossil of the so-called Penrich Sandstone (*M. geslinianum* Zone) in Saxony (Häntzschel 1933). Nevertheless, based on the macrofaunal data, the Cenomanian-Turonian boundary cannot be precisely determined in the boreholes due to lack of any index species at the C-T boundary or its poor preservation.

The stratigraphically important foraminiferal species *Gavelinella cenomanica* Brotzen indicates a Cenomanian age for these samples. A relatively poor foraminiferal assemblage with rare occurrences of planktonic species of the genera *Whiteinella (W. archaeocretacea)* and *Hedbergella* make it possible to assign the strata to the planktonic *Whiteinella archaeocretacea* Interval and the Partial-range Zone (from the upper part of Upper Cenomanian to the lowermost part of the Lower Turonian) sensu Robaszynski and Caron (1995). A more diverse Early Turonian foraminiferal assemblage is represented by the *Helvetoglobotruncana helvetica* Zone (Robaszynski and Caron 1995) due to the occurrence of *H. helvetica*. The first occurrence of *H. helvetica* is correlated with the first occurrence of the calcareous nannofossil marker species *Eprolithus moratus* (Figs 2 and 3).

The last occurrence of the nannofossil species *Corollithion kennedyi* defines the UC3d-e Subzone boundary (lower Upper Cenomanian, Burnett 1998). The rare presence of this species in borehole Nymburk HP-20 is interpreted as having been reworked from the underlying strata. Conversely, *Lithraphidites acutus* may be interpreted as an autochthonous component. Its last occurrence defines the UC4-UC5 zone boundary, located within the stratigraphic interval of the Plenus Marls (*M. geslinianum* Zone, Burnett 1998). *Axopodorhabdus albianus* is a common component of Cenomanian nannofossil assemblages. Its last occurrence is a significant datum marking the UC5a-b Subzone boundary, located within the upper part of the Plenus Marls (*M. geslinianum* Zone, Burnett 1998, Paul et al. 1999).

The uppermost Cenomanian, the interval between the last occurrence of *Axopodorhabdus albianus* and the influx of Turonian nannoflora (probably equivalent to the *juddii* Zone), was identified only in the Hořátev HP-19 borehole

VELKÉ ZBOŽÍ BJ-17	Lower Turonian						
Standard nannofossil zones Sissingh (1977), Perch-Nielsen (1985)	CC10b				CC11		
Upper Cretaceous nannofossil zones Burnett (1998)	UC5c–UC6a			UC6b	UC7		
depth (m)	103.2	102.3	100.8	95.1	90.1	85.0	82.5
samle abundance	H	H	H	H	H	H	H
nannofossil preservation	M	M	M	M	M	M	M
Biscutum ellipticum	R	F	F	F	F	F	F
Broinsonia enormis	R	F	F	C	F	F	F
Broinsonia signata	R			F		F	F
Eiffellithus gorkae	F	R	F	F	F	F	
Eiffellithus turriseeiffelii	F	F	F	C	C	F	C
Eprolithus apertior	R						
Eprolithus floralis	F	F	F	F	F	F	F
Eprolithus octopetalus	R	R			F		
Gartnerago obliquum	F	F	F	F	R	F	F
Grantarhabdus coronadventis	F	R	R		R	F	F
Haqius circumradiatus	R		R	R			
?Helenea chiastia	R	R					R
Helicolithus compactus	R	R					
Helicolithus trabeculatus	F	F	F	F	F	F	F
Lithraphidites carniolensis	R		R	F	R	R	R
Manivitella pemmatoidea	F	R	F	R	R	F	F
Prediscosphaera columnata	C	F	F	F	R	R	R
Prediscosphaera cretacea	F	F	C	F	C	C	A
Prediscosphaera ponticula	F	F	C	F	F	R	F
Quadrum giganteum	R	R	R	F			
Quadrum intermedium (7 ray-like elements)	R		VR				VR
Retacapsa angustiforata	R		F	F	F	F	
Retacapsa crenulata	R				F	R	F
Rhagodiscus angustus	R	R		R	R	F	F
Tranolithus gabalus	R	F				R	R
Tranolithus orionatus	F	R	F	F	F		
Watznaueria barnesae	VA	VA	VA	VA	VA	VA	VA
Watznaueria biporta	R		R	R			
Zeugrhabdotus diplogrammus	C	C			R		
Zeugrhabdotus embergerii	F	R	C	C	C	C	A
Zeugrhabdotus noeliae	C	C	F				
Zeugrhabdotus trivectis	F	F	F	C	F	F	
Amphizygus brooksii		R	R	R	F		
Chiastozygus litterarius		R	F	F	F	F	
Cretarhabdus conicus		F	F	F	F		
Placozygus cf. *fibuliformis*		F	F	F	F	F	R
Prediscosphaera spinosa		R	R	R	R	R	R
Rhagodiscus splendens		R		F	F	R	F
Stoverius achylosus		R	R	R	F	F	F
Watznaueria fossacincta		R		VR	R	F	R
Loxolithus sp.		R	R				
Zeugrhabdotus bicrescenticus		R	F		F	R	F
Broinsonia matalosa			VR		VR		
Cribrosphaerella ehrenbergii			R	F	F	F	F

VELKÉ ZBOŽÍ BJ-17	Lower Turonian						
Standard nannofossil zones Sissingh (1977), Perch-Nielsen (1985)	CC10b				CC11		
Upper Cretaceous nannofossil zones Burnett (1998)	UC5c–UC6a			UC6b	UC7		
depth (m)	103.2	102.3	100.8	95.1	90.1	85.0	82.5
Lucianorhabdus cf. maleformis			R	R		F	
Rotelapillus crenulatus			F	R	F	F	F
Scapholithus fossilis			VR	VR			
Tranolithus minimus			VR				
Ahmuellerella octoradiata				F	F	F	F
Corollithion signum				R		F	R
Eprolitus moratus				F	F	F	F
Lapideacassis sp.				VR	R		
Quadrum gartneri				R	R		
Quadrum intermedium (5 ray-like elements)					VR		
Staurolithites laffittei					R		
Corollithion signum						VR	
Eprolithus rarus (6 elements)						VR	
Octolithus cf. *multiplus*						R	
?*Rhagodiscus plebeius*						F	
Sollasites horticus						VR	
Watznaueria britannica						R	R
Braarudosphaera bigelowii							R
Microrhabdulus belgicus							R

Figure 10. Calcareous nannofossil distribution in the Velké Zboží BJ-17 borehole. For explanations see Fig. 8.

(Fig. 2). Its short vertical range, or even its absence (Nymburk HP-20 borehole – see Fig. 3), may indicate an interruption of the otherwise continuous deposition, which is also suggested by a prominent marine erosion surface and a high content of glauconite and phosphates in the basal glauconitic bed of the Bílá Hora Formation (Figs 2, 3 and 15). In this interval, only agglutinated foraminifers appear. The foraminiferal assemblages are impoverished, and the calcareous tests of forams are decalcified.

The appropriate marker species to recognize the Turonian beds seems to be the nannofossil species *Eprolithus octopetalus,* the first occurrence of which is known from the lowermost Turonian (Burnett 1998). Nevertheless, the chronostratigraphic position of this datum remains obscure. Luciani and Cobianchi (1999) reported its occurrence in zone CC11, in the lower part of the *Helvetoglobotruncana helvetica* Zone. Burnett (1998) mentioned *E. octopetalus* at the base of subzone UC6b, and the range of zone CC11 approximately correlates with Zone UC7. The short interval between the first occurrences of *Eprolithus octopetalus* and *E. moratus* is regarded as a stratigraphically important datum comparable to the *Watinoceras devonense* ammonite Zone, the lowermost part of the Turonian (Burnett 1998). Inoceramids of *Mytiloides* ex gr. *labiatus* also occur at this level (Hořátev HP-19 borehole, 105.7 m).

Discussion

Fluvial, estuarine to shallow marine deposits were recorded from cores of the Peruc-Korycany Formation with palynomorph assemblages that correlate with the sedimentological interpretations. Similar palynomorph assemblages were found in the Pecínov quarry (Uličný et al. 1997a). In the lower part of the fluvial facies in borehole HP-20 (depth 150.3 m), a small percentage of acritarchs was found besides the typical continental palynologic assemblage that, as in the Pecínov quarry, indicates an influx of marine water upstream.

In the restricted marine facies assemblages, halophyte pollen of *Classopollis/Corollina* is a characteristic feature that indicates that their parent plants (derived from *Frenelopsis alata*, Cheirolepidicaeae, Hluštík and Konzalová 1976) were important components of the coastal marshes (Batten 1975). Batten (1982) found a direct correlation between increased numbers of cheirolepidiacean pollen and transgressive phases. A similar trend is evident through the fluvial to estuarine succession in borehole HP-20, associated with an increased number of dinocysts (Fig. 3). The diversity of dinocysts is usually low, and the association often consists of species tolerant of salinity changes, i.e. *Odontochitina operculata* or peridinioid type *Subtilisphaera perlucida.* Marine coastal to shallow shelf envi-

VELKÉ ZBOŽÍ BJ-18	Lower Turonian						
Standard nannoplankton zones Sissingh (1977), Perch-Nielsen (1985)	CC10b		CC11				
Upper Cretaceous nannofossil zones Burnett (1998)	UC5c–UC6a				UC7		
depth (m)	106.3	105.5	102.4	98.4	93.9	88.0	83.0
sample abudance	H	H	H	M	M	M	H
nannofossil preservation	M	M	M	P	P	P	M
Amphizygus brooksii	F	R	R	R		R	
Biscutum ellipticum	C	F	C	C	F	R	F
Bronsonia enormis	F	F	F	F	F	F	F
Chiastozygus litterarius	F	F	F	F	R	R	R
Cretarhabdus conicus	F	F	F	R	R	R	R
Eiffellithus turriseiffelii	F	F	C	C	C	F	C
Eprolithus floralis	R	F	F	R	R	R	F
Eprolithus octopetalus	F	R	F				
Gartnerago obliquum	R	F	F	R	F	F	F
Grantarhabdus coronadventis	R	R	F	F		R	R
?Helenea chiastia	VR						
Helicolithus compactus	R	R	F		R	R	F
Helicolithus trabeculatus	C	F	F	F	F	F	F
Lithraphidites carniolensis	R	R	R	R	R		R
Manivitella pemmatoidea	R	R	R	R	R	R	R
Prediscosphaera columnata	F	F	F	R	R	R	R
Prediscosphaera cretacea	C	C	C	F	C	C	C
Prediscosphaera ponticula	F	F	F	R	R	R	R
Quadrum intermedium (7 ray-like elements)	R			VR			
Retacapsa angustiforata	F	R	R	F	R	R	
Retacapsa ficula	VR		R		VR		
Rhagodiscus angustus	R	R	F	R	R	F	
Rhagodiscus asper	R			R		R	
Rotelapillus crenulatus	F	F	F	F	F	R	R
Tranolithus gabulus	F	R		R	R	F	R
Tranolithus orinatus	A	C	C	C	C	A	C
Watznaueria barnesae	VA	VA	VA	VA	VA	VA	VA
Watznaueria biporta	R	R			R	R	R
Watznaueria fossacincta	R				R	R	
Zeugrhabdotus bicrescenticus	R	F	R	R	R	F	F
Zeugrhabdotus diplogrammus	R	R	R	R	F		
Zeugrhabdotus noeliae	C	C	F	F		R	R
Zeugrhabdotus trivectis	F	F	R	F	R	R	
Corollithion signum		R	F		R		R
Cribrosphaerella ehrenbergii		R	R	F	R	R	R
Haqius circumradiatus		R		F			
Placozygus cf. *fibuliformis*		R	F	R	R	R	R
Retacapsa crenulata		F	R			R	R
Rhagodiscus splendens		R	R	R	R	R	R
Stoverius achylosus		F			R	R	R
Watznaueria britannica		R			R	R	
Ahmuellerella octoradiata			R	R	C	F	F
Broinsonia signata			R	F	F	F	
Eprolithus moratus			F	F	F	F	F

VELKÉ ZBOŽÍ BJ-18	Lower Turonian						
Standard nannoplankton zones Sissingh (1977), Perch-Nielsen (1985)	CC10b		CC11				
Upper Cretaceous nannofossil zones Burnett (1998)	UC5c–UC6a				UC7		
depth (m)	106.3	105.5	102.4	98.4	93.9	88.0	83.0
Lucianorhabdus cf. *maleformis*			R	R	R	F	R
Quadrum gartneri			R				
Sollasites horticus			VR				
Staurolithites laffittei			R	VR		R	
Tranolithus minimus			VR		VR		
Eprolithus apertior				VR			
Prediscosphaera spinosa				R		R	R
Braarudosphaera bigelowii					R		R
Lapideacassis sp.					R		
Octolithus ?multiplus					R		
Quadrum intermedium (5 ray-like elements)					VR	R	
Corollithion exiguum							VR
Octocyclus reinhardtii							R

Figure 11. Calcareous nannofossil distribution in the Velké Zboží BJ-18 borehole. For explanations see Fig. 8.

ronments yield dinocysts from the littoral group *Circulodinium,* the neritic group I – *Spiniferites,* and neritic group II – *Oligosphaeridium* and *Florentinia* (Wilpshaar and Leereveld 1994, Leereveld 1995). The relative abundance of ceratiacean (*Odontochitina*), peridiniacean (*Palaeohystrichophora*), and rare gonyaulacacean (*Oligosphaeridium*) groups indicate proximity to the shore, and are a useful salinity index. The increase of peridiniaceaen dinocysts indicates reduced salinity, whereas gonyaulacacean cysts are associated with offshore, open marine conditions (Davey 1970, Harland 1973, Batten 1979). Some studies (Wall 1965) have shown that acanthomorph acritarchs (i.e., *Micrhystridium*) are commonly associated with an inshore, restricted basinal environment. Many prasinophycean algae are considered to be euryhaline, and thus common in tidal pools and brackish water (Tappan 1980). Foraminiferal test-linings are useful environmental indicators because they are common in marine coastal to shallow shelf environments (Batten 1979). Miospores are also commonly more numerous than microplankton in near-shore deposits. The isolated record of gymnosperm pollen *Ephedripites* and *Araucariacites* is an indicator of arid/semiarid environments (Ibrahim and Schrank 1996). Ephedroid pollen characterises a Tethyan realm, while in the Boreal realm deposits are rarely encountered.

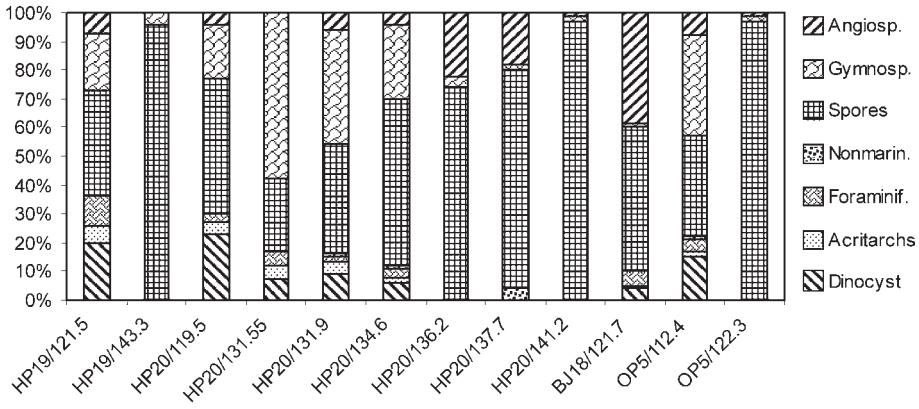

Figure 12. Distribution of dinocysts, acritarchs, non-marine plankton, spores, and pollen in productive samples of HP-19, HP-20, BJ-18 and OP-5 boreholes from the Poděbrady area.

The rare occurrences of agglutinated foraminifera species of *Trochammina, Bigenerina, Ammobaculoides*, and *Ataxophragmium* were recorded in non-calcareous heterolithic sediments from the Korycany Member. These foraminifers were probably able to tolerate the paralic environment with lower salinity (Koutsoukos and Hart 1990). Palynomorph assemblages from these beds (HP-20, sample 119.5 m) exhibit features similar to estuarine tidal flat and channel facies associations, but with a considerably higher content of dinocysts. It seems that the heterolithic intercalations in the Korycany sandstones were deposited in an intertidal to shallow subtidal environment, probably at the mouth of the estuary.

The dinocyst species *Epelidosphaeridia spinosa* (formerly regarded as Middle Cenomanian – the *E. spinosa* Subzone of Davey, 1970) occurs in some samples (HP-19: 121.5 m, HP-20: 119.5 m, BJ-18: 121.7 m, OP-5: 112.4 m). Robaszynski et al. (1988) and Paul et al. (1994) reported its occurrence also in the upper part of Lower Cenomanian (*Mantelliceras dixoni* Zone) and Middle Cenomanian (*Acanthoceras rhotomagense* Zone) in northwest Europe.

Boreholes No.	HP-19		HP-20									BJ-18	OP-5	
sample No./depth (m)	HP19/121.5	HP19/143.3	HP20/119.5	HP20/131.55	HP20/131.9	HP20/134.6	HP20/136.2	HP20/137.7	HP20/141.2	HP20/142.9	HP20/150.3	BJ18/121.7	OP5/122.3	OP5/112.4
Dinoflagellate cysts														
Achomosphaera ramulifera			x	x										
Callaiosphaeridium assymetricum														
Canningia sp.				x										
Cleistosphaeridium spp.	x				xx	x						xx		
Circulodinium distinctum	x		x		xx	xx						xx		xx
Epelidosphaeridia spinosa	xx		xx	x								xx		xx
Florentinia mantelii														x
Odontochitina operculata														x
Oligosphaeridium complex	x													
Palaeohystrichophora infusorioides			x			x								x
Pervosphaeridium pseudhystrichodinium						x								
Spiniferites ramosus	xx		xx		xx	x						x		xx
Surculosphaeridium ? longifurcatum	x													x
Xenascus ceratioides														x
Acritarcha and Prasinophyta														
Cymatiosphaera sp.	x					x		x				x		
Micrhystridium fragile					xx	xx								x
Micrhystridium spp.	xx		xx	x	x	xx								
Veryhachium hyalodermum				x										x
Non-marine algae Zygnemataceae														
Chomotriletes minor						x		xx	xx					
Ovoidites parvus					x	x		xx				xx		x
Paralecaniella sp.								xx				x		
Tetraporina sp.														x
Bryophyte and pteridophyte spores														
Biretisporites potoniei		x				x								
Calamospora sp.													x	
Camarozonosporites ambigens				xx	xx	xx	●					x		
Camarozonosporites insignis	xx		xx	xx	xx	xx		●						xx
Cicatricosisporites venustus	x	xx		x		xx						xx		
Cicatricosisporites sp.		xx						xx			x			
Cingutriletes clavus					xx			xx						
Clavifera triplex		x				x							xx	
Coronatispora sp.				xx				x						
Deltoidospora minor	xx	xx	x		x		xx		xx				xx	
Foveogleicheniidites confossus		xx					xx		x					
Foveotriletes subtriangularis						x								
Gleicheniidites carinatus							x	x					xx	
Gleicheniidites circiniidites												xx		
Gleicheniidites senonicus	●			xx		○	○	○	●	x	●	xx	●	●
Laevigatosporites ovatus					x	●	●	●	●			x		
Leptolepidites psarosus		xx			x								x	
Matonisporites sp.												x		
Microfoveolatosporites canaliculatus							x					x	x	
Ornamentifera echinata									x			x	xx	

Boreholes No.	HP-19		HP-20									BJ-18	OP-5	
sample No./depth (m)	HP19/121.5	HP19/143.3	HP20/119.5	HP20/131.55	HP20/131.9	HP20/134.6	HP20/136.2	HP20/137.7	HP20/141.2	HP20/142.9	HP20/150.3	BJ18/121.7	OP5/122.3	OP5/112.4
Plicatella spp.			xx						xx	x		xx		x
Reticulosporites sp.		x												
Retitriletes austroclavatidites			xx	xx	xx			x						xx
Sestrosporites pseudoalveolatus							x							
Stereisporites antiquasporites	xx		xx	xx	●		○		●			xx		xx
Stereisporites psilatus			xx				xx		xx					
Undulatisporites sp.						x								
Vadaszisporites urkuticus						x	x							
Gymnosperm pollen grains														
Alisporites bilateralis						xx						○		
Araucariacites cf. *australis*						x								
Classopollis classoides	●	x	xx	○	○	x								○
Cycadopites fragilis						xx			●					
Ephedripites jansonii						x								
Ephedripites multicostatus												x		
Eucommiidites minor						xx			xx					
Inaperturopollenites sp.		x			xx	x		x						
Parvisaccites radiatus	xx				x	●	xx		x		xx	○		xx
Phyllocladidites sp.						x								
Pinuspollenites sp.					xx	xx	x		x					
Sequoiapollenites sp.											x	x		
Taxodiaceaepollenites hiatus	xx		xx	xx	xx	○	xx	x	●		xx	○	x	○
Taxodiaceaepollenites vacuipites						xx			x					
Angiosperm pollen grains														
Bohemiperiporis zaklinskae					x		xx							
Brenneripollis peroreticulatus							xx	xx						
Clavatipollenites minutus					xx		xx	x						x
Complexiopollis sp.														x
aff. *Foveotetradites fistulosus*									xx					
Foveotricolpites sp.			x											x
Liliacidites sp. A						xx						x		x
Perucipollis minutus							●	xx	○				x	
Psilatricolpites parvulus	xx		x			xx	xx	xx					x	
Psilatricolporites sp.									xx					
Retitricolpites micromunus			xx				xx		●					
Retitricolpites němejci														
Retitricolpites virgeus									x					
Retitricolpites vulgaris			xx				xx							
Retitricolpites spp.					xx	xx	xx	xx	x	x		x		xx
Retitricolporites spp.	xx											x	xx	x
aff. *Stephanocolpites* sp.									x					
Tricolpites barrandei					x		xx		xx					
Tricolpites crassimurus								x						
Tricolpites cf. sagax						x								

Figure 13. Relative abundances of the main palynomorph groups through the HP-19, HP-20, BJ-18, OP-5 borehole sequences.
x – rare, xx – common (2–10 specimen), ● – abundant (11–25 specimen), ○ – frequent (more than 26 specimens)

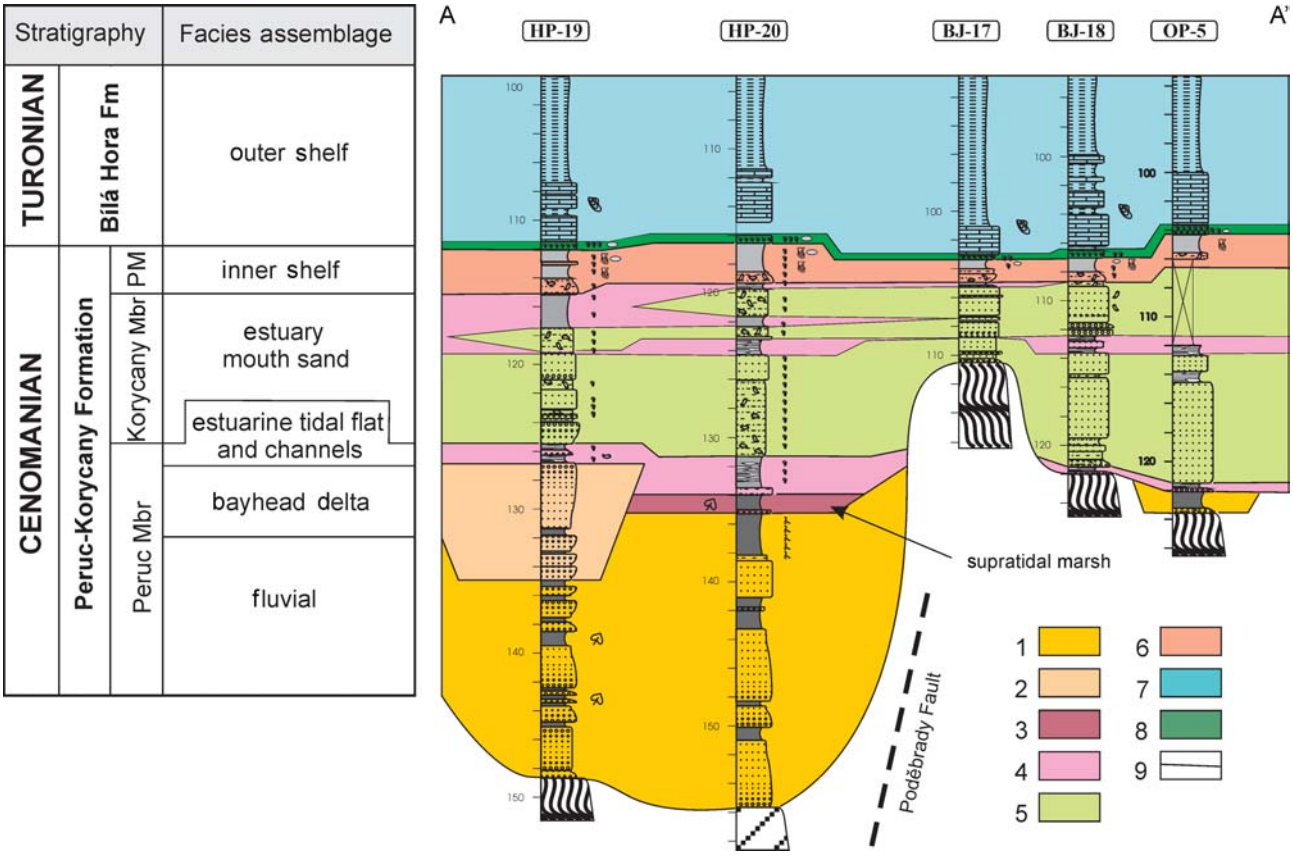

Figure 14. Stratigraphic cross section A–A´ of the Poděbrady area and facies assemblages, illustrating transgessive character of Cenomanian-Turonian sequence. Location of the cross section A–A´ is shown in Fig. 1C. Incised-valley fill and paleoelevation is shown. Heterolithic bed within Korycany Formation was chosen as key bed. For lithology see explanations on Fig. 2.
1 – fluvial facies, 2 – estuarine bayhead delta facies, 3 – supratidal marsh facies, 4 – estuarine tidal flat and channels facies, 5 – estuarine and mouth sand facies, 6 – inner shelf facies, 7 – open shelf facies, 8 – glauconitic bed, 9 – bounding surfaces, PM – Pecínov Member.

In Spain, *E. spinosa* was reported from the Upper Cenomanian above the first occurrence of planktonic foraminifers of *Helvetoglobotruncana praehelvetica*, and just below the first appearance of bivalve species *Mytiloides submytiloides* by Mao and Lamolda (1998). According to a recent study by Svobodová (unpublished), *E. spinosa* was found in the calcareous siltstones of the Pecínov Member in borehole Dolní Bousov DB-1, from the northern part of the BCB, together with *Praeactinocamax plenus* (Upper Cenomanians *M. geslinianum* Zone).

The biostratigraphically important angiosperm pollen *Complexiopollis* spp. from the Normapolles Group appears in sample OP-5 (from 112.4 m), and it may correspond with the upper part of the Korycany Member. According to Laing (1975), Durand and Louail (1976), Pacltová (1977), Louail et al. (1978), and Méon et al. (2004) the first primitive *Complexiopollis* pollen (three pores are often unclear) are found in the *jukes-brownei* Zone, Middle Cenomanian, but the earliest occurrence of true Normapolles, represented by the genera *Complexiopollis* and *Atlantopollis*, are known from the Upper Cenomanian (Solé de Porta 1978, Méon et al. 2004).

In the cores, stratigraphically important foraminifers and nannofossils were obtained only from calcareous siltstones of the uppermost part of the Cenomanian (Pecínov Member), and from the marlstones and micritic limestones of the Turonian Bílá Hora Formation.

The foraminiferal assemblage of the Pecínov Member consists mostly of agglutinated and calcareous benthos with the stratigraphically important *Gavelinella cenomanica*. The appearance of *Gavelinella cenomanica* in this region provides evidence for the local development of calcareous Cenomanian sediments, which are characteristic for the central part of the BCB between Mělník and Benátky n. J., where *G. cenomanica* is abundant (Hradecká 1993, Uličný et al. 1993).

The foraminiferal assemblage of the Upper Cenomanian Pecínov Member was set to the planktonic *Whiteinella archaeocretacea* Interval and Partial-range Zone sensu Robaszynski and Caron (1995). The presence of the planktonic *Rotalipora cushmani* Zone (the uppermost part of the Middle Cenomanian to the lower part of the Upper Cenomanian) was not recorded due to the very sporadic occurrence or absence of *Rotalipora cushmani* in the Cenomanian sediments of the BCB (see also discussion in Uličný et al. 1993).

In the literature, the Cenomanian-Turonian boundary is not clearly defined by the first occurrence of any nannofossil species. Some authors have mentioned the first occurrence of *Quadrum gartneri* in the lowermost Turonian (Lamolda et al. 1994, Luciani and Cobianchi 1999,

Paul et al. 1999, and others), though Burnett (1998) records its first occurrence in the upper part of the Lower Turonian. Polycycloliths of the genus *Quadrum*, having four large ray-like elements of equal size, and one to three small ray-like elements in each cycle of the wall, were also included as *Q. gartneri* up to 1992 when Varol (1992) described them as a new species, *Quadrum* intermedium. In the studied material, both *Quadrum gartneri* and *Q. intermedium* were observed in very low numbers in Turonian deposits, and they are suitable neither for the precise zonation nor for the determination of Cenomanian-Turonian boundary. For instance, species *Q. intermedium* (5 elements) was found in Hořátev HP-19 borehole at a depth of 110.9 m, in association with *Eprolithus octopetalus*. Nevertheless, rare *Q. intermedium* occurrences (introduced as *Q. gartneri* by Hradecká et al. 1997) were recorded from the uppermost Cenomanian of the nearby borehole Kouty BJ-16.

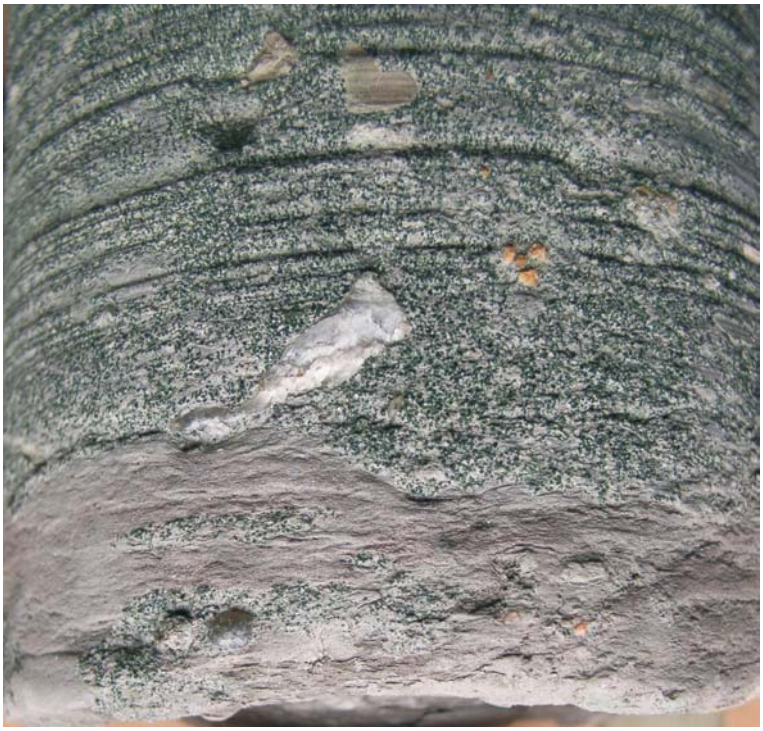

Figure 15. Core photo from borehole Sokoleč OP-3, core interval 63.1–63.25 m. Erosion surface at the base of green glauconitic sandy marlstone (base of Bílá Hora Fm.) with pebbles of quartz and phosphatic nodules. *Thallassinoides* burrows pipe glauconitic sediment down into the underlying dark grey siltstones of the Pecínov Member. Core is stored at CGS.

According to Roth and Krumbach (1986), the positive correlation of the C_{org} content of the sediment and the relative abundance of *Watznaueria barnesae* indicate carbonate dissolution caused by the release of carbon dioxide during the oxidation of organic matter. Assemblages with more than 40 % of *W. barnesae* are probably highly dissolved and secondarily enriched in this species. This phenomenon was observed especially in the Cenomanian, where low-diversity nannofossil assemblages are secondarily modified by carbonate dissolution. It is supported not only by higher percentage of *W. barnesae*, but also by the mode of coccolith preservation and by the absence of some "subtle" species of Stephanolithiaceae. In contrast, nannofossils in basal Turonian strata are well preserved, diversified, and small in size, though the abundance of *W. barnesae* is also high. Similar nannofossils, remarkably small in size but of a different age (Upper Turonian and Coniacian), were observed in the marine transgressive deposits of the Lower Gosau-Subgroup, Northern Calcareous Alps (Hradecká et al. 1999). In the overlying strata, the percentage of *W. barnesae* decreases slightly, while the sizes of nannofossils return to the standard form. The abundance and higher species diversity of the latter, along with the relatively common occurrence of "subtle" specimens of the family Stephanolithiaceae, may evince relatively settled marine depositional environments.

Conclusions

The following conclusions can be drawn from the foregoing discussion:

1. An incised valley filled by Cenomanian fluvial and estuarine sediments and paleoelevation was recognized in studying new and older boreholes. This paleovalley was a side tributary of the main Cenomanian depression in the central part of the BCB.
2. The sedimentary sequence of the Peruc-Korycany (Cenomanian) Formation shows an overall transgressive character from fluvial through estuarine, and up to inner shelf environment. The transgressive character of the sedimentary sequence was interpreted according to the succession of facies assemblages and the flora and fauna distribution in drill core samples.
3. The following depositional environments were recognized according to facies assemblages in the Peruc-Korycany Formation: fluvial facies, estuarine bayhead delta, supratidal marsh facies, estuarine tidal flat and channel facies, estuarine and mouth sand facies, and inner marine facies.
4. A transgressive succession from fluvial to supratidal marsh to estuarine tidal flat facies is well documented in Nymburk HP-20 borehole by the gradual increase of halophyte gymnosperm pollen and dinocysts that tolerate salinity changes, as well as by a decrease in the numbers of pteridophyte spores (Fig. 3).
5. In the general transgressive/regressive order through the Cenomanian–Turonian sequence, there are transgressive/regressive sequences of smaller orders, interrupted by major or prominent bounding surfaces associated with erosional surface and stratigraphic condensation of the uppermost Cenomanian strata. The gradual deepening into open shelf facies is documented by the increasing diversity of foraminifer and calcare-

Figure 16. Correlation of foraminifers and calcareous nannofossils. Interval of stratigraphic condensation is marked in grey.

ous nannoplankton assemblages in the overlying hemipelagic sediments of Turonian age.

6. Based on the triporate angiosperm pollen Complexiopollis, the age of most of the studied samples from the Peruc and Korycany members correspond to the Middle to Upper Cenomanian. *Epelidosphaeridia spinosa* occurs from the Middle Cenomanian up to the Upper Cenomanian. In the BCB, this species was found also in siltstones yielding *Preactinocamax plenus* (*Metoicoceras geslinianum* Zone).
7. Biostratigraphically, the Upper Cenomanian marine strata can be subdivided into two parts according to the last occurrence of the nannofossil species *Axopodorhabdus albianus*. The lower part (zones ?UC4–UC5a) represented by calcareous siltstones of the Pecínov Member correlates approximately with the lower part of the Plenus Marl (*M. geslinianum* Zone). The upper part [zones UC5b–UC5c (lower part)] is represented by the glauconitic bed of the base of Bílá Hora Formation, and is separated from the lower part by a prominent erosion surface. This interval is correlated with the *Neocardioceras juddii* Zone, and probably with the uppermost part of the *M. geslinianum* Zone (Fig. 16).
8. The interval from the first occurrence of the nannofossil species *Eprolithus octopetalus* to the first occurrence of *Eprolithus moratus* (zones UC5c–UC6a) in the hemipelagic micritic limestones of the lower part of the Bílá Hora Formation coincides approximately with the *Watinoceras devonense* Zone, which is delineated within the lowermost part of Turonian.
9. The first occurrence of *Eprolithus octopetalus* falls into the *Whiteinella archaeocretacea* Interval and the Partial-range Zone. In lower part of the Bílá Hora Formation, the first occurrence of *Eprolithus moratus* coincides with the first appearance of foraminiferal planktonic species *Helvetoglobotruncana helvetica* (Fig. 16).

References

Batten D. J. (1975): Wealden palaecology from the distribution of plant fossils. Proc. Geol. Assoc. 85, 433–458.

Batten D. J. (1979): Miospores and other acid-resistant microfossils from the Aptian/Albian of Holes 400A and 402A, DSDP-IPOD Leg 48 Bay of Biscay. In: Initial Reports of the Deep Sea Drilling Project, 48. U.S. Government Printing Office, Washington, D. C., 579–587.

Batten D. J. (1982): Palynofacies and salinity in the Purbeck and Wealden of southern England. In: Banner F. T., Lord A. R. (eds) Aspects of micropalaeontology. London, 278–308.

Burnett J. A. (1998): Upper Cretaceous. In: Bown P. R. (ed.) Calcareous nannofossil biostratigraphy. Cambridge University Press, Cambridge, 132–199.

Čech S. (2004): Křídová výplň poděbradské zřídelní struktury. Zpr. geol. Výzk. v Roce 2003, 20–21 (in Czech with English abstract).

Čech S., Klein V., Kříž J., Valečka J. (1980): Revision of Upper Cretaceous Stratigraphy of the Bohemian Cretaceous Basin. Věst. Ústř. Úst. geol. 55, 277–296.

Davey R. J. (1970): Non-calcareous microplankton from the Cenomanian of England, northern France and North America. Part II. Bull. Br. Mus. (Nat. Hist.), Geol. 18, 33–397.

Durand S., Louail J. (1976): Intérét stratigraphique du sondage de Loudun (Vienne) pour l'étude du Cénomanien de l'ouest de la France. C. R. Hebd. Seances. Acad. Sci., Série D 283, 1719–1722.

Eliášová H. (1997): Coraux crétacé de Boheme (Cenomanien supérieur; Turonien inférieur–Coniacien inférieur), République tchèque. Bull. Czech Geol. Surv. 72, 3, 245–266.

Frejková L., Vajdík J. (1974): Příspěvek k paleogeografii a litologii cenomanských sedimentů v orlicko-žďárské faciální oblasti. Sbor. GPO 8, 5–28 (in Czech).

Häntzschel W. (1933): Das Cenoman und die Plenus-Zone der sudetischen Kreide. Abh. Peuss. Geol. Landesant., NF. 150, 1–161.

Harland R. (1973): Dinoflagellate cysts and acritarchs from the Bearpaw Formation (Upper Campanian) of southern Alberta, Canada. Paleontology 16, 665–706.

Hercogová J. (1968): Strukturní vrty OP-1 až OP-6 na Poděbradsku. Zpráva o mikrobiostratigrafickém vyhodnocení svrchní křídy. In: Hruška J., Kolářová M., Krásný J., Müller V., Vodička J. (eds) Podklady pro ochranná pásma lázní Poděbrad. Hydrogeologie Poděbradska a návrh ochrany lázní Poděbrad. Unpub. Czech Geological Survey – Geofond, Prague (in Czech).

Hluštík A., Konzalová M. (1976): Polliniferous cones of Frenelopsis alata (K. Feistm.) Knobloch from the Cenomanian of Czechoslovakia. Věst. Ústř. Úst. geol. 51, 37–45.

Hradecká L. (1993): Changes of foraminiferal assemblages and related events of the Late Cenomanian to Early turonian in the central part of the Bohemian Cretaceous Basin. Acta Univ. Carol., Geol. 3–4, 19–22.

Hradecká L., Lobitzer H., Ottner F., Sachsenhofer R. F., Siegl-Farkas A., Švábenická L., Zorn I. (1999): Biostratigraphy and Palaeoenvironment of the marly marine transgression of Weißenbachalm Lower Gosau-Subgroup (Upper Turonian-Lower Santonian Grabenbach-Formation, Northern Calcareous Alps, Styria). Abh. Geol. B.-A. 56, 2, 475–517.

Hradecká L., Pražák J., Švábenická L. (1997): Předběžné vyhodnocení vrtu Kouty BJ-16 (česká křídová pánev). Zpr. geol. Výzk. v Roce 1996, 113–115 (in Czech).

Hradecká L., Švábenická L. (1995): Foraminifera and Calcareous Nannoplankton assemblages from the Cenomanian-Turonian boundary interval of the Knovíz Section, Bohemian Cretaceous Basin. Geol. Carpath. 46, 5, 267–276.

Hruška J., Kolářová M., Krásný J., Müller V., Vodička J. (1968): Podklady pro ochranná pásma lázní Poděbrad. Hydrogeologie Poděbradska a návrh ochrany lázní Poděbrad. Unpub. Czech Geological Survey – Geofond, Prague (in Czech).

Ibrahim M., Schrank E. (1996): Palynological studies on the Jurassic-Early Cretaceous of the Kahraman-1 well, Northern Western desert, Egypt. Géologie de l'Afrique et de l'Atlantique Sud: Actes Colloques Angers 1994, 611–629.

Klein V. (1966): Stratigrafie a litologie svrchní křídy mezi Jizerou a Labem. Sbor. geol. Věd, Geol. 11, 49–75 (in Czech with German abstract).

Klein V., Hercogová J., Rejchrt M. (1982): Stratigraphie, Lithologie und Paläontologie der Kreide im Elbe-Faziesgebiet. Sbor. geol. Věd, Geol. 36, 27–92.

Klein V., Müller V., Valečka J. (1979): Lithofazielle und paläogeographische Entwicklung des Böhmischen Kreidebeckens. Aspekte der Kreide Europas. IUGS Series A 6, 425–446.

Koutsoukos E. A. M., Hart M. B. (1990): Cretaceous foraminiferal morphogroup distribution patterns, palaeocommunities and trophic structures: a case study from the Sergipe Basin, Brazil. Trans. R. Soc. Edinb.-Earth Sci. 81, 221–246.

Laing J. F. (1975): Mid-Cretaceous angiosperm pollen from Southern England and Northern France. Paleontology 18, 4, 775–808.

Lamolda M. A., Gorostidi A., Paul C. R. C. (1994): Quantitative estimates of calcareous nannofossil changes across the Plenus Marls (latest Cenomanian), Dover, England: implications for the generation of the Cenomanian-Turonian boundary event. Cretac. Res. 15, 143–164.

Leereveld H. (1995): Dinoflagellate cysts from the Lower Cretaceous Río Argos succession (SE Spain). Lab. Palaeobot. Palynol. Contr. Ser. 2, 1–175.

Louail J., Bellier J. P., Damotte R., Durand S. (1978): Stratigraphie du Cénomanien littoral de la marge Sud-Ouest du Bassin de Paris. L'example du sondage de Loudun. Géol. Méditer. 5, 1, 115–124.

Luciani V., Cobianchi M. (1999): The Bonarelli Level and other black shales in the Cenomanian-Turonian of the northeastern Dolomites (Italy): calcareous nannofossil and foraminifera data. Cretac. Res. 20, 135–167.

Mao S., Lamolda M. A. (1998): Quistes dinoflagelados del Ceno-

maniense superior y Turoniense inferior de Ganuza, Navara. I – Paleontología sistemática. Rev. Esp. Paleontol. 13, 2, 261–286.
Méon H., Guignard G., Pacltová B., Svobodová M. (2004): Normapolles. Comparaison entre l'Europe centrale et du Sud-Est pendant le Cénomanien et le Turonien: évolution de la biodiversité et paléoenvironnement. Bull. Soc. géol. Fr. 175, 6, 579–593.
Pacltová B. (1977): Cretaceous angiosperms of Bohemia – Central Europe. Bot. Rev. 43, 1, 128–142.
Pacltová B., Svobodová M. (1993): Facial characteristics from palynological point of view in the area of the Bohemian Cenomanian. Proc. Symposium Paleofloristic and Paleoclimatic changes during Cretaceous and Tertiary, September 1992 Bratislava, Konf., Symp., Semináre, Geol. úst. D. Štúra, 17–21.
Paul C. R. C., Lamolda M. A., Mitchell S. F., Vaziri M. R., Gorostidi A., Marshall J. D. (1999): The Cenomanian-Turonian boundary at Eastbourne (Sussex, UK): a proposed European reference section. Paleogeogr. Paleoclimatol. Paleoecol. 150, 83–121.
Paul C. R. C., Mitchell S. F., Marshall J. D., Leary P. N., Gale A. S., Duane A. M., Ditchfield P. W. (1994): Palaeoceanographic events in the Middle Cenomanian of Northwest Europe. Cretac. Res. 15, 707–738.
Perch-Nielsen K. (1985): Mesozoic calcareous nannofossils. In: Bolli H. M., Saunders J. B., Perch-Nielsen K. (eds) Plankton stratigraphy. Cambridge Univ. Press, Cambridge, 329–426.
Pražák J. (1989): Hranice cenoman–turon v centrální části české křídové pánve. Unpub. Czech Geological Survey, Prague (in Czech).
Robaszynski F., Alcaydé G., Amédro F., Badille G., Damotte R., Foucher J.-C., Jardiné S., Legoux O., Manivit H., Moncardini Ch., Sornay J. (1988): Le Turonien de la region-Type: Saumurois et Touraine, Stratigraphie, Biozonations, Sédimentologie. Bull. Centres Rech. Explor., Prod. El-Aquitaine 6, 1, 119–225.
Robaszynski F., Caron M. (1995): Foraminifčres planctoniques du Crétacé commentaire de la zonation Europe – Méditerranée. Bull. Soc. Géol. France 166, 6, 681–692.
Roth P. H., Krumbach K. P. (1986): Middle Cretaceous calcareous nannofossil biogeography and preservation in the Atlantic and Indian Oceans: Implications for paleoceanography. Mar. Micropaleontol. 10, 235–266.
Sissingh W. (1977): Biostratigraphy of Cretaceous calcareous nannoplankton. Geol. Mijnb. 56, 37–65.
Solé de Porta N. (1978): Palynology of two Cenomanian sections near Oviedo, Spain. Palinologia, Núm. Extraord. 1, 435–441.
Soukup J., Vodička J. (1967): Strukturní vrt do podloží křídy v Sobčicích u Jičína (KN-5). Zpr. geol. Výzk. v Roce 1967, 194–196 (in Czech).
Svoboda P. (1998): Transgrese svrchní křídy mezi Kralupy nad Vltavou a Korycany. Studie Okres. muz. Praha-východ 13, 129–154 (in Czech).
Svobodová M. (1990): Lower Turonian microflora at Skalka near Velim (Central Bohemia, CSFR). Bull. Czech Geol. Surv. 65, 5, 291–300.
Svobodová M., Méon H., Pacltová B. (1998): Characteristics of the Upper Cenomanian–Lower Turonian (anoxic facies) of the Bohemian and Vocontian Basins. Bull. Czech Geol. Surv. 73, 3, 229–251.
Štemproková-Jírová D. (1991): Biostratigraphy of planktic foraminifera from the Cenomanian and Turonian of the locality Velim (Bohemian Cretaceous Basin, Czechoslovakia). Acta Univ. Carol., Geol. 1–2, 103–125.
Švábenická L. (2004): Bohemian Cretaceous Basin – Cenomanian-Turonian boundary based on calcareous nannofossils. Zpr. geol. Výzk. v Roce 2003, 44–47 (in Czech with English abstract).
Tappan H. (1980): The paleobiology of plant protists. W. H. Freemann & Comp., San Francisco.
Uličný D. (1992): Low and high-frequency sea-level change and related events during the Cenomanian and across the Cenomanian-Turonian boundary, Bohemian Cretaceous Basin. Unpub. Thesis Charles Univ., Prague.
Uličný D. (1997): Sedimentation in a reactivated, intra-continental strike-slip fault zone: The Bohemian Cretaceous Basin, Central Europe. Gaea heidelbergensis, 3, Abstracts, 18th IAS Regional European Meeting, Heidelberg, 347.
Uličný D. (2001): Depositional systems and sequence stratigraphy of coarse-grained deltas in a shallow-marine, strike-slip setting: the Bohemian Cretaceous Basin, Czech Republic. Sedimentology 48, 599–628.
Uličný D., Hladíková J., Hradecká L. (1993): Record of sea level changes, oxygen depletion and the C anomaly across the Cenomanian – Turonian boundary, Bohemian Cretaceous Basin. Cretac. Res. 14, 211–234.
Uličný D., Kvaček J., Svobodová M., Špičáková L. (1997a): High frequency sea-level fluctuations and plant habitats in Cenomanian fluvial to estuarine succession: Pecínov quarry, Bohemia. Palaeogeogr., Palaeoclimatol., Palaeoecol. 136, 165–197.
Uličný D., Hladíková J., Attrep M., Čech S., Hradecká L., Svobodová M. (1997b): Sea-level changes and geochemical anomalies across the Cenomanian-Turonian boundary: Pecínov quarry, Bohemia. Paleogeogr. Paleoclimatol. Paleoecol., 132, 265–285.
Uličný D., Špičáková L., Čech S. (2003): Changes in depositional style of an intra-continental strike-slip basin in response to shifting activity of basement fault zones: Cenomanian of the Bohemian Cretaceous Basin. Geolines 16, 103–104.
Varol O. (1992): Taxonomic revision of the Polycyclolithaceae and its distribution to Cretaceous biostratighraphy. Newsl. Stratigr. 27, 3, 93–127.
Wall D. (1965): Microplankton, pollen, and spores from the Lower Jurassic in Britain. Micropaleontology 11, 2, 151–190.
Wilpshaar M., Leereveld H. (1994): Palaeoenvironmental change in the Early Cretaceous Vocontian Basin (SE France) reflected by dinoflagellate cysts. Rev. Palaeobot. Palynol. 84, 121–128.
Žítt J., Nekvasilová O., Bosák P., Svobodová M., Štemproková-Jírová D., Šťastný M. (1997a): Rocky coast facies of the Cenomanian-Turonian Boundary interval at Velim (Bohemian Cretaceous Basin, Czech Republic). First part. Bull. Czech Geol. Surv. 72, 1, 83–100.
Žítt J., Nekvasilová O., Bosák P., Svobodová M., Štemproková-Jírová D., Šťastný M. (1997b): Rocky coast facies of the Cenomanian-Turonian Boundary interval at Velim (Bohemian Cretaceous Basin, Czech Republic). Second part. Bull. Czech Geol. Surv. 72, 2, 141–155.

Appendix

Macrofauna taxa mentioned in the text

Cephalopoda
Praeactinocamax plenus (Blainville)

Bivalvia
Apiotrigonia sulcataria (Lamarck)
Chlamys robinaldina (D'Orbigny)
Neithea notabilis (Münster)
Perna cretacea Reuss
Pseudoptera anomala (Sowerby)
Rastellum carinatum (Lamarck)

Foraminiferal taxa mentioned in the text, in alphabetical order of genera epithets
Ammobaculites reophacoides Bertenstein
Ammobaculoides lepidus Hercogová
Ammodiscus cretaceus (Reuss)
Ammodiscus gaultinus Berthelin
Arenobulimina preslii (Reuss)
Ataxophragmium depressum (Perner)
Bigenerina selseyensis Heron-Allen-Earland
Cassidella tegulata (Reuss)
Dentalina sp.
Dicarinella imbricata (Mornod)
Dorothia filiformis (Berthelin)
Dorothia gradata (Berthelin)
Dorothia oxycona (Reuss)
Dorothia turris (d'Orbigny)
Frondicularia sp.
Frondicularia fritschi Perner
Frondicularia inversa Reuss
Frondicularia verneuiliana d'Orbigny
Gaudryina angustata Akimec
Gaudryina compressa Akimec
Gaudryina folium Akimec
Gaudryina praepyramidata Hercogová

Gaudryina trochus (d'Orbigny)
Gaudryina variabilis Mjatljuk
Gavelinella baltica Brotzen
Gavelinella belorussica (Akimec)
Gavelinella berthelini (Keller)
Gavelinella cenomanica (Brotzen)
Gavelinella polessica Akimec
Gavelinella schloenbachi (Reuss)
Gyroidina nitida (Reuss)
Hagenowina advena (Cushman)
Haplophragmoides sp.
Haplophragmoides nonioninoides (Reuss)
Haplophragmoides ovalis Jendrejáková
Haplophragmoides stelcki Hanzlíková
Hedbergella delrioensis (Carsey)
Hedbergella planispira (Tappan)
Hedbergella simplex (Morrow)
Helvetoglobotruncana helvetica (Bolli)
Helvetoglobotruncana praehelvetica (Trujillo)
Heterohelix globulosa (Ehrenberg)
Heterohelix pulchra Brotzen
Lenticulina sp.
Lenticulina comptoni (Sowerby)
Lingulogavelinella globosa (Brotzen)
Lingulogavelinella pazdroae Gawor-Biedowa
Lituotuba incerta Franke
Marginulina aequivoca Reuss
Marginulina robusta (Reuss)
Marssonella oxycona (Reuss)
Nodosaria sp.
Nodosaria bistegia (Olszewski)
Nodosaria obscura (Reuss)
Planularia complanata (Reuss)
Praebulimina crebra Štemproková
Praeglobotruncana delrioensis (Plummer)
Praeglobotruncana oraviensis Scheibnerová
Pseudotextularia cretosa (Cushman)
Quadrimorphina allomorphinoides (Reuss)
Ramulina globulifera Brady
Spiroplectammina sp.
Spiroplectammina scotti Cushman-Alexander
Tappannina eouvigeriniformis (Keller)
Textularia foeda Reuss
Trochammina sp.
Trochammina globosa Bolin
Trochammina obliqua Tappan
Vaginulina recta Reuss
Vaginulina robusta (Chapman)
Valvulineria lenticula (Reuss)
Whiteinella aprica (Loeblich & Tappan)
Whiteinella archaeocretacea Pessagno
Whiteinella baltica Douglas & Rankin
Whiteinella brittonensis (Loeblich & Tappan)
Whiteinella paradubia (Sigal)

Nannofossil taxa mentioned in the text, in alphabetical order of genera epithets
Ahmuellerella octoradiata (Górka) Reinhardt
Amphizygus brooksii Brooksii
Axopodorhabdus albianus (Black) Wind and Wise
Biscutum ellipticum (Górka) Grün
Braarudosphaera bigelowii (Gran and Braarud) Deflandre
Broinsonia enormis (Shumenko) Manivit
Broinsonia matalosa (Stover) Burnett
Broinsonia signata (Noël) Noël
Bukrylithus ambiguus Black
Chiastozygus litterarius (Górka) Manivit
Corollithion exiguum Stradner
Corollithion kennedyi Crux
Corollithion signum Stradner
Cretarhabdus conicus Bramlette and Martini
Cribrosphaerella ehrenbergii (Arkhangelsky) Deflandre
Cyclagelosphaera rotaclypeata Bukry
Eiffellithus turriseiffelii (Deflandre) Reinhardt
Eprolithus floralis (Stradner) Stover
Eprolithus moratus (Stover) Burnett
Eprolithus octopetalus Varol
Gartnerago obliquum (Stradner) Noël
Gartnerago theta (Black) Jakubowski
Grantarhabdus coronadventis (Reinhardt) Grün
Haqius circumradiatus (Stover) Roth
Helenea chiastia Worsley
Helicolithus compactus (Bukry) Varol and Girgis
Helicolithus trabeculatus (Górka) Verbeek
Isocrystallithus compactus Verbeek
Lithraphidites acutus Verbeek and Manivit
Lithraphidites carniolensis Deflandre
Lucianorhabdus maleformis Reinhardt
Manivitella pemmatoidea (Deflandre) Thierstein
Microrhabdulus belgicus Hay and Towe
Microrhabdulus decoratus Deflandre
Nannoconus elongatus Brönnimann
Perissocyclus fenestratus (Stover) Black
Placozygus fibuliformis (Reinhardt) Hoffmann
Prediscosphaera columnata (Stover) Perch-Nielsen
Prediscosphaera cretacea (Arkhangelsky) Gartner
Prediscosphaera ponticula (Bukry) Perch-Nielsen
Prediscosphaera spinosa (Bramlette and Martini) Gartner
Quadrum gartneri Prins and Perch-Nielsen
Quadrum intermedium Varol
Retacapsa angustiforata Black
Retacapsa crenulata (Bramlette and Martini) Grün
Rhagodiscus angustus (Stradner) Reinhardt
Rhagodiscus asper (Stradner) Reinhardt
Rhagodiscus plebeius Perch-Nielsen
Rhagodiscus splendens (Deflandre) Verbeek
Rotelapillus crenulatus (Stover) Perch-Nielsen
Stoverius achylosus (Stover) Perch-Nielsen
Tegumentum stradneri Thierstein
Tranolithus gabalus Stover
Tranolithus orionatus (Reinhardt) Reinhardt
Watznaueria barnesae (Black) Perch-Nielsen
Watznaueria biporta Bukry
Watznaueria britannica (Stradner) Reinhardt
Watznaueria fossacincta (Black) Bown
Zeugrhabdotus bicrescenticus (Stover) Burnett
Zeugrhabdotus diplogrammus (Deflandre) Burnett
Zeugrhabdotus embergeri (Noël) Perch-Nielsen
Zeugrhabdotus erectus (Deflandre) Reinhardt
Zeugrhabdotus noeliae Rood et al.
Zeugrhabdotus scutula (Bergen) Rutledge and Bown
Zeugrhabdotus trivectis Bergen
Zeugrhabdotus xenotus (Stover) Burnett

Palynomorph taxa mentioned in the text, in alphabetical order of genera epithets
Achomosphaera ramulifera (Deflandre) Evitt
Alisporites bilateralis Rouse
Araucariacites cf. *australis* Cookson
Biretisporites potoniei Delcourt & Sprumont
Bohemiperiporis zaklinskae Pacltová
Brenneriporis peroreticulatus (Brenner) Juhász & Góczán
Callaiosphaeridium asymmetricum (Deflandre & Courteville) Davey & Williams
Calamospora sp.
Camarozonosporites ambigens (Fradkina) Playford
Camarozonosporites insignis Norris
Canningia sp.
Chomotriletes minor Pocock
Cicatricosisporites venustus Deák
Cicatricosisporites sp.
Cingutriletes clavus (Balme) Dettmann
Circulodinium distinctum (Deflandre & Cookson) Jansonius
Classopollis /Corollina/ classoides (Pflug) Pocock & Jansonius
Clavatipollenites minutus Brenner
Clavifera triplex (Bolchovitina) Bolchovitina

Cleistosphaeridium sp.
Complexiopollis sp.
Coronatispora sp.
Cycadopites fragilis Singh
Cyclonephelium compactum Deflandre & Cookson
Cymatiosphaera sp.
Deltoidospora minor (Couper) Pocock
Dyadosporites ellipsus Clarke
Epelidosphaeridia spinosa Cookson & Hughes
Ephedripites jansonii (Pocock) Muller
Ephedripites multicostatus Brenner
Eucommiidites minor Couper
Florentinia mantelii (Davey & Williams) Davey & Verdier
Foveogleicheniidites confossus (Hedlund) Burger
aff. *Foveotetradites fistulosus* (Dettmann)
Foveotricolpites sp.
Foveotriletes subtriangularis Brenner
Gleicheniidites carinatus (Bolchovitina) Bolchovitina
Gleicheniidites circiniidites (Cookson) Dettmann
Gleicheniidites senonicus Ross
Inaperturopollenites sp.
Laevigatosporites ovatus Wilson & Webster
Leptolepidites psarosus Norris
Liliacidites sp. A
Matonisporites sp.
Microfoveolatosporites canaliculatus Dettmann
Micrhystridium fragile Deflandre
Micrhystridium spp.
Odontochitina operculata (O. Wetzel) Deflandre & Cookson
Oligosphaeridium complex (White) Davey & Williams
Ornamentifera echinata Bolchovitina
Ovoidites parvus (Cookson & Dettmann)
Palaeohystrichophora infusorioides Deflandre
Paralecaniella sp.
Parvisaccites radiatus Couper
Perucipollis minutus Pacltová
Pervosphaeridium pseudhystrichodinium (Deflandre) Yun
Phyllocladidites sp.
Pinuspollenietes spp.
Plicatella ethmos (Delcourt & Sprumont) Zhang
Plicatella sp.
Psilatricolpites parvulus (Groot & Penny) Norris
Psilatricolporites sp.
Reticulosporites sp.
Retitricolpites micromunus (Groot & Penny) Burger
Retitricolpites němejci (Pacltová) Laing
Retitricolpites virgeus (Groot, Penny & Groot) Brenner
Retitricolpites vulgaris Pirce
Retitricolpites spp.
Retitricolporites spp.
Retitriletes austroclavatidites (Cookson) Döring et al.
Sequoiapollenites sp.
Sestrosporites pseudoalveolatus (Cooper) Dettmann
Spiniferites ramosus (Ehrenberg) Loeblich & Loeblich ssp. *ramosus* aff.
Stephanocolpites sp.
Stereisporites antiquasporites (Wilson & Webster) Kremp
Stereisporites psilatus (Ross)
Surculosphaeridium ?longifurcatum (Firtion) Davey
Taxodiaceaepollenites hiatus (potonié) Kremp
Taxodiaceaepollenites vacuipites Kremp
Tetracolpites sp.
Tetraporina sp.
Tricolpites barrandei Pacltová
Tricolpites crassimurus (Groot & Penny) Singh
Tricolpites cf. *sagax* Norris
Undulatisporites sp.
Vadaszisporites urkuticus Juhász
Veryhachium hyalodermum (Cookson) Downie & Sarjeant
Xenascus ceratioides (Deflandre) Lentin & Williams

→

Plate I
1 — *Valvulineria lenticula* (Reuss), umbilical side, BJ-20, 113.5 m. 2 – *Helvetoglobotruncana helvetica* (Bolli), BJ-19, 110.9 m. 3 – *Valvulineria lenticula* (Reuss), spiral side, BJ-19, 110.9 m. 4 – *Gavelinella polessica* Akimec, BJ-20, 113.5 m. 5 – *Ramulina* sp., BJ-20, 113.5 m. 6 – *Gavelinella belorussica* (Akimec), BJ-19, 110.9 m. 7 – *Praebulimina crebra* Štemproková, BJ-20, 113.5 m. 8 – *Praebulimina crebra* Štemproková, BJ-19, 110.9 m. 9 – *Heterohelix pulchra* Brotzen, BJ-19, 110.9 m. 10 – *Gavelinella cenomanica* (Brotzen), Cenomanian, BJ-20, 116.7 m. 11 – *Gavelinella cenomanica* (Brotzen), Cenomanian, BJ-20, 116.7 m. 12 – *Ataxophragmium depressum* (Perner), BJ-20, 116.7 m.

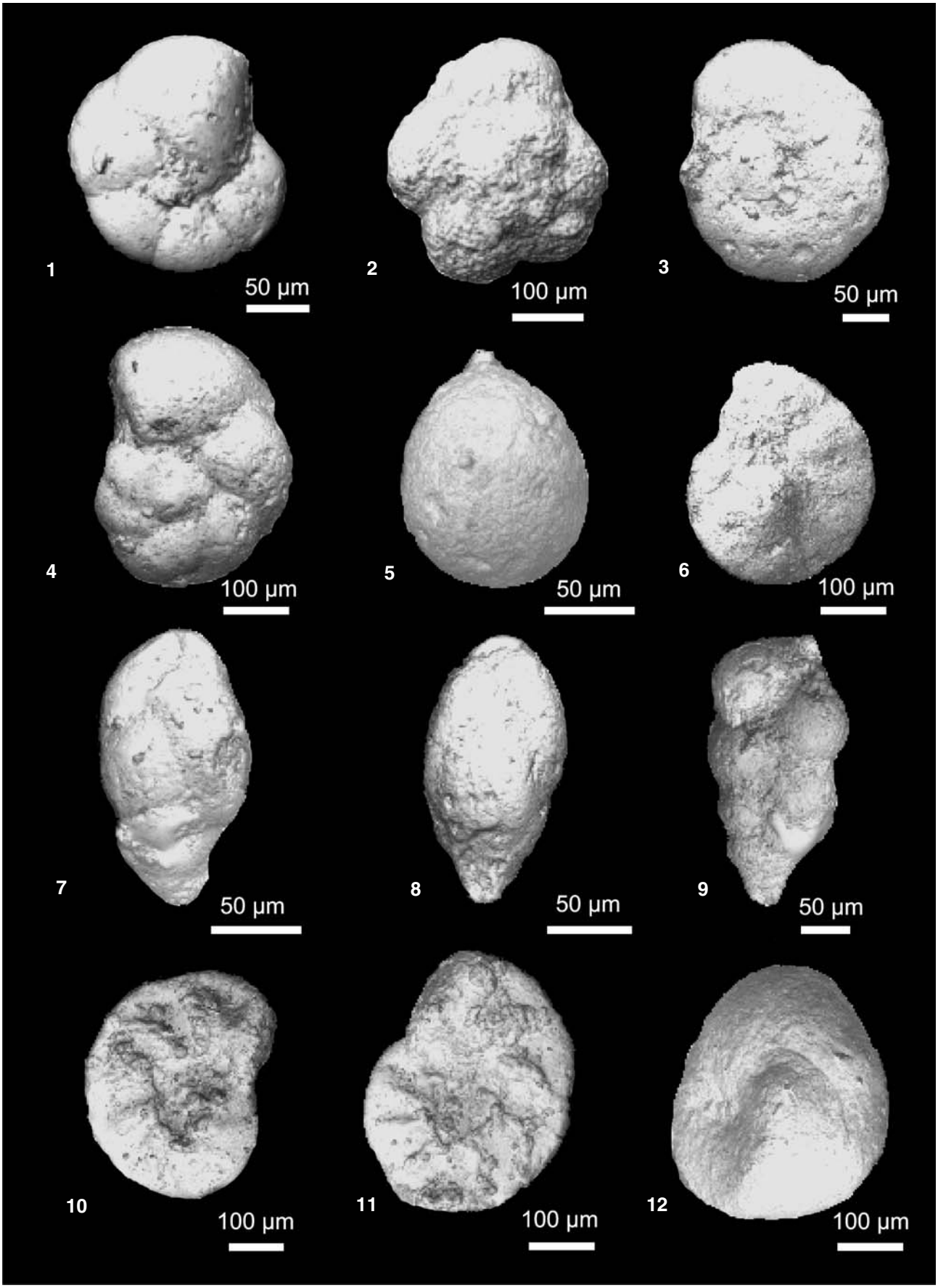
1
50 µm
2
100 µm
3
50 µm
4
100 µm
5
50 µm
6
100 µm
7
50 µm
8
50 µm
9
50 µm
10
100 µm
11
100 µm
12
100 µm

→

Plate II
1 – *Valvulineria lenticula* (Reuss), umbilical side, BJ-19, 110.9 m. 2 – *Lingulogavelinella globosa* (Brotzen), BJ-19, 110.9 m. 3 – *Gavelinella cenomanica* (Brotzen), BJ-20, 116.7 m. 4 – *Heterohelix pulchra* Brotzen, BJ-19, 110.9 m. 5 – *Haplophragmoides* sp., BJ-20, 116.7 m. 6 – *Trochammina obliqua* Tappan, BJ-20, 121.9 m. 7 – *Ammobaculites lepidus* Hercogová, BJ-20, 121.9 m. 8 – *Trochammina obliqua* Tappan, BJ-20, 121.9 m. 9 – *Praebulimna crebra* Štemproková, BJ-19, 110.9 m. 10 – *Cassidella tegulata* (Reuss), BJ-20, 113.5 m.

→→

Plate III
Calcareous nannofossils from the Cenomanian-Turonian boundary interval, Nymburk HP-20 borehole (if not otherwise indicated), Bohemian, Cretaceous Basin. PPL – plane-polarized light, XPL – cross-polarized light.
1, 2 – *Broinsonia enormis* (Shumenko) Manivit, Lower Turonian, 111.4 m, 1, PPL, 2, XPL. 3, 4 – *Broinsonia signata* (Noël) Noël, Upper Cenomanian, 117.0 m, 3, PPL, 4, XPL. 5, 6 – *Helicolithus trabeculatus* (Górka) Verbeek, Upper Cenomanian, 116.7 m, 5, PPL, 6, XPL. 7 – *Biscutum ellipticum* (Górka) Grün, Upper Cenomanian, 117.0 m, XPL. 8-10 – *Prediscosphaera columnata* (Stover) Perch-Nielsen, Upper Cenomanian, 117.0 m, 8,9, PPL, 10, XPL. 11, 12 – *Prediscosphaera spinosa* (Bramlette and Martini) Gartner, Lower Turonian, 111.4 m, 11, PPL, 12, XPL. 13–15 – *Prediscosphaera ponticula* (Bukry) Perch-Nielsen, Upper Cenomanian, 13, 14: 116.7 m, 13, PPL, 14, XPL, 15, 117.0 m, XPL. 16–18 – *Axopodorhabdus albianus* (Black) Wind and Wise, Upper Cenomanian, 16, 17: 116.7 m, 16, PPL, 17, XPL, 18, 117.0 m, XPL. 19–21 – *Eiffellithus turriseiffelii* (Deflandre) Reinhardt, Upper Cenomanian, 117.0 m, 19, PPL, 20, 21, XPL. 22, 23 – *Quadrum intermedium* Varol, Lower Turonian, Hořátev HP-19 borehole, 106.3 m, 22, PPL, 23, XPL. 24 – *Quadrum gartneri* Prins and Perch-Nielsen, Lower Turonian, Hořátev HP-19 borehole, 101.9 m, XPL. 25–28 – *Eprolithus floralis* (Stradner) Stover, Upper Cenomanian, 117.0 m, 25, 27, PPL, 26, 28, XPL. 29, 30 – *Eprolithus octopetalus* Varol, Lower Turonian, 116.4 m, 29, PPL, 30, XPL. 31–33 – *Eprolithus moratus* (Stover) Burnett; Lower Turonian, 111.4 m, 31, 32, PPL, 33, XPL. 34–36 – *Eprolithus* sp., lateral view; 34: Lower Turonian, 116.4 m, PPL, 35, 36: Upper Cenomanian, 117.4 m, 35, PPL, 36, XPL.

→→→

Plate IV
Calcareous nannofossils from the Cenomanian-Turonian boundary interval, Nymburk HP-20 borehole, Bohemian Cretaceous Basin. PPL – plane-polarized light, XPL – cross-polarized light.
1, 2 – *Corollithion kennedyi* Crux, Upper Cenomanian, 117.0 m, XPL. 3, 4 – *Stoverius achylosus* (Stover) Perch-Nielsen, Lower Turonian, 116.4 m, 3, PPL, 4, XPL. 5, 6 – *Zeugrhabdotus noeliae* Rood et al., Upper Cenomanian, 117.0 m, 5, PPL, 6, XPL. 7, 8 – *Gartnerago theta* (Black) Jakubowski, Upper Cenomanian, 117.0 m, 7, PPL, 8, XPL. 9 – *Gartnerago obliquum* (Stradner) Noël, Lower Turonian, 111.4 m, XPL. 10 – *Zeugrhabdotus trivectis* Bergen, Upper Cenomanian, 116.7 m, XPL. 11 – *Zeugrhabdotus bicrescenticus* (Stover) Burnett, Upper Cenomanian, 116.3 m, XPL. 12 – *Amphizygus brooksii* Bukry, Upper Cenomanian, 117.0 m, XPL. 13, 14 – *Tranolithus orionatus* (Reinhardt) Reinhardt, Upper Cenomanian, 117.0 m, 13, PPL, 14, XPL. 15, 16 – *Chiastozygus litterarius* (Górka) Manivit, Lower Turonian, 116.4 m, 15, PPL, 16, XPL. 17 – *Watznaueria britannica* (Stradner) Reinhardt, Upper Cenomanian, 117.0 m, XPL. 18 – *Watznaueria barnesae* (Black) Perch-Nielsen, Lower Turonian, 111.4 m, XPL. 19, 20 – *Retacapsa* sp.; Lower Turonian, 111.4 m, 19, PPL, 20, XPL. 21, 22 – *Retacapsa angustiforata* Black, Upper Cenomanian, 116.7 m, 21, PPL, 22, XPL. 23 – *Retacapsa crenulata* (Bramlette and Martini) Grün, Upper Cenomanian, 117.0 m, XPL. 24 – *Braarudosphaera bigelowii* (Gran and Braarud) Deflandre, Lower Turonian, 113.5 m, XPL. 25 – *Haqius circumradiatus* (Stover) Roth, Lower Turonian, 111.4 m, PPL. 26 – *Nannoconus elongatus* Brönnimann, Upper Cenomanian, 117.4 m, PPL. 27 – ?*Isocrystallithus compactus* Verbeek, Lower Turonian, probably reworked specimen from the underlying strata, 111.4 m, XPL. 28, 29 – *Lucianorhabdus maleformis* Reinhardt, Lower Turonian, 111.4 m, 28, PPL, 29, XPL. 30 – *Lucianorhabdus* cf. *L. maleformis* (sensu Burnett 1998), Lower Turonian, 111.4 m, XPL. 31, 32 – *Manivitella pemmatoidea* (Deflandre) Thierstein, Upper Cenomanian, 117.0 m, 31, PPL, 32, XPL. 33, 34 – *Lithraphidites acutus* Verbeek and Manivit, Upper Cenomanian, 117.0 m, 33, PPL, 34, XPL. 35, 36 – *Lithraphidites* cf. *L. acutus*, Upper Cenomanian, 117.0 m, 35, PPL, 36, XPL.

→→→→
Plate V
Palynomorphs from the Middle–Upper Cenomanian interval of the borehole Nymburk HP-20. Micrographs by M. Svobodová.
1 – *Perucipollis minutus* Pacltová, 134.60 m, 1243/2. 2 – *Bohemiperiporis zaklinskae* Pacltová, 136.20 m, 1244/2. 3 – *Tetracolpites* sp., 141.20 m, 1246/5. 4 – *Retitricolpites vulgaris* Pierce, 141.20 m, 1246/1. 5 – *Foveotetradites fistulosus* (Dettmann) Singh, tetrahedral tetrad, 141.20 m, 1246/3. 6 – *Retitricolporites* sp., 137.70 m, 1245/2. 7 – *Liliacidites* sp., 134.60 m, 1243/2. 8 – *Laevigatosporites ovatus* Wilson & Webster, 143.30 m, 1241/1. 9 – *Classopollis classoides* (Pflug) Pocock & Jansonius, 131.90 m, 1242/3. 10 – *Ephedripites jansonii* (Pocock) Muller, 137.70 m, 1245/1. 11 – *Tricolpites* cf. *sagax* Norris, 134.60 m, 1243/2. 12 – *Eucommiidites minor* Couper, 134.60 m, 1243/3. 13 – *Paralecaniella* sp., 137.70 m, 1245/1. 14 – *Chomotriletes minor* Pocock, 134.60 m, 1243/2. 15 – *Dyadosporites ellipsus* Clarke, 134.60 m, 1243/2. 16 – *Plicatella ethmos* (Delcourt & Sprumont) Zhang, 143.30 m, 1241/1. 17 – Foraminiferal linings, 134.60 m, 1243/2. 18 – *Cyclonephelium compactum* Deflandre & Cookson, 134.60 m, 1243/3.

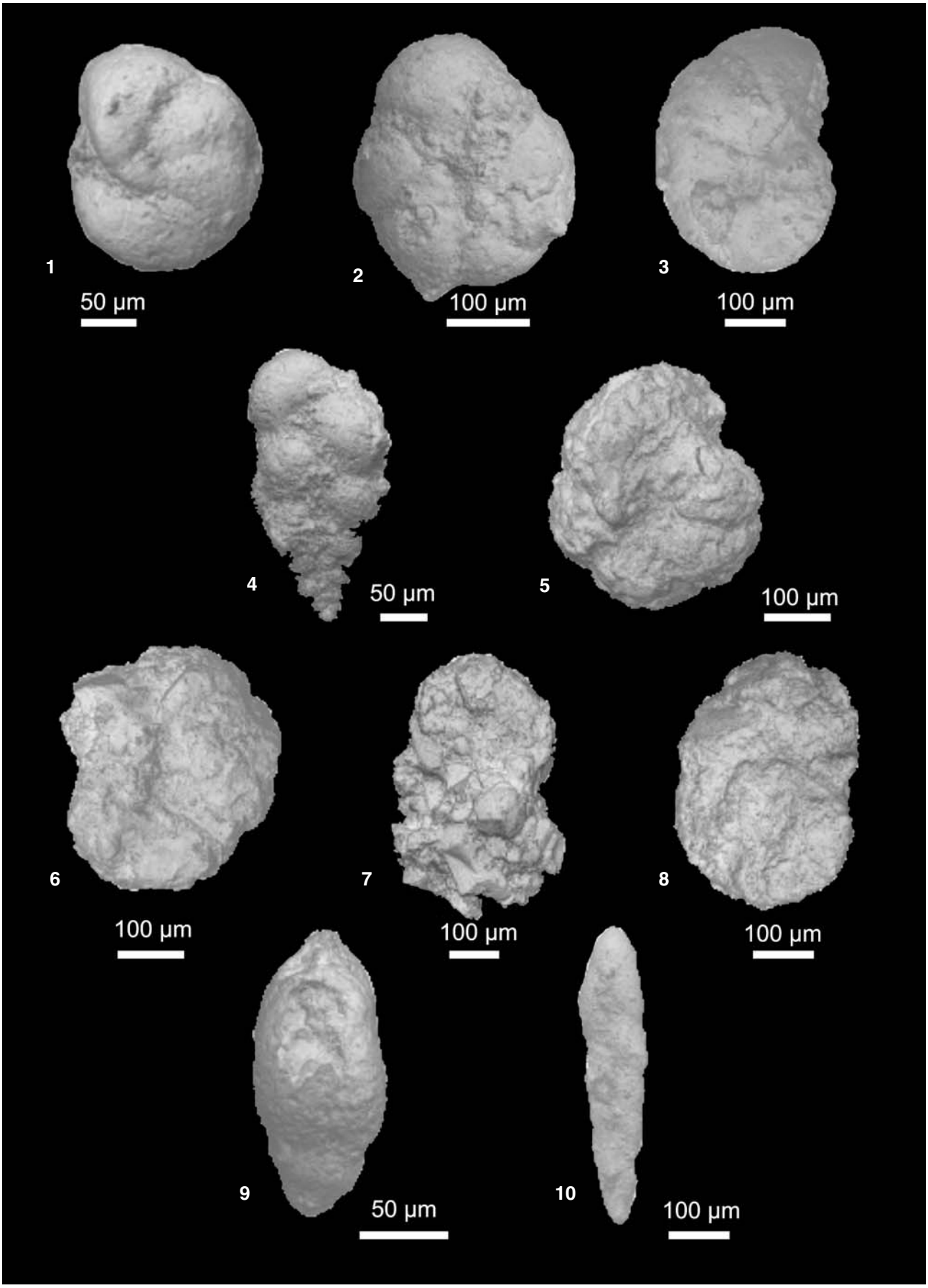
1
50 µm
2
100 µm
3
100 µm
4
50 µm
5
100 µm
6
100 µm
7
100 µm
8
100 µm
9
50 µm
10
100 µm

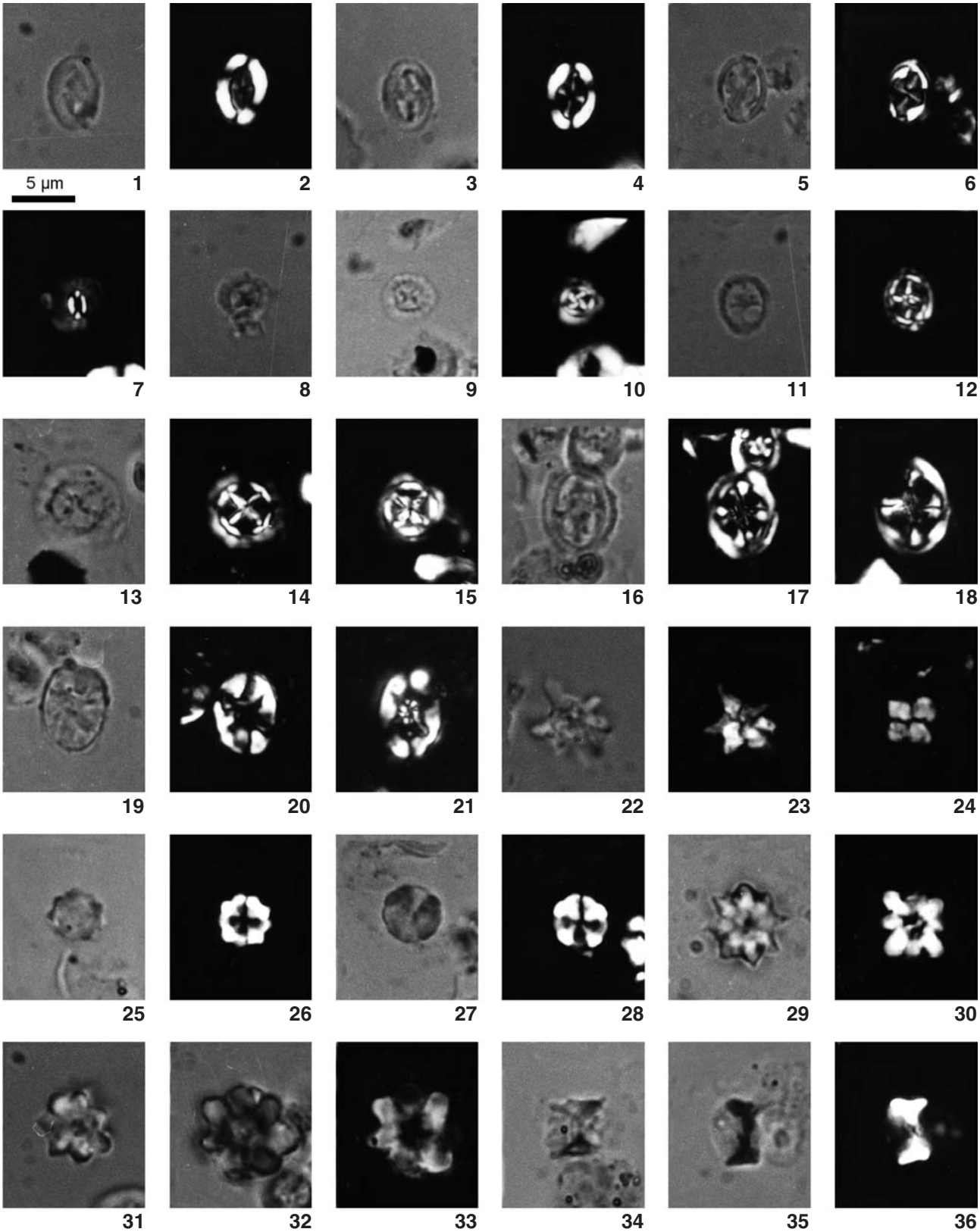
5 µm
1
2
3
4
5
6
7
8
9
10
11
12
13
14
15
16
17
18
19
20
21
22
23
24
25
26
27
28
29
30
31
32
33
34
35
36

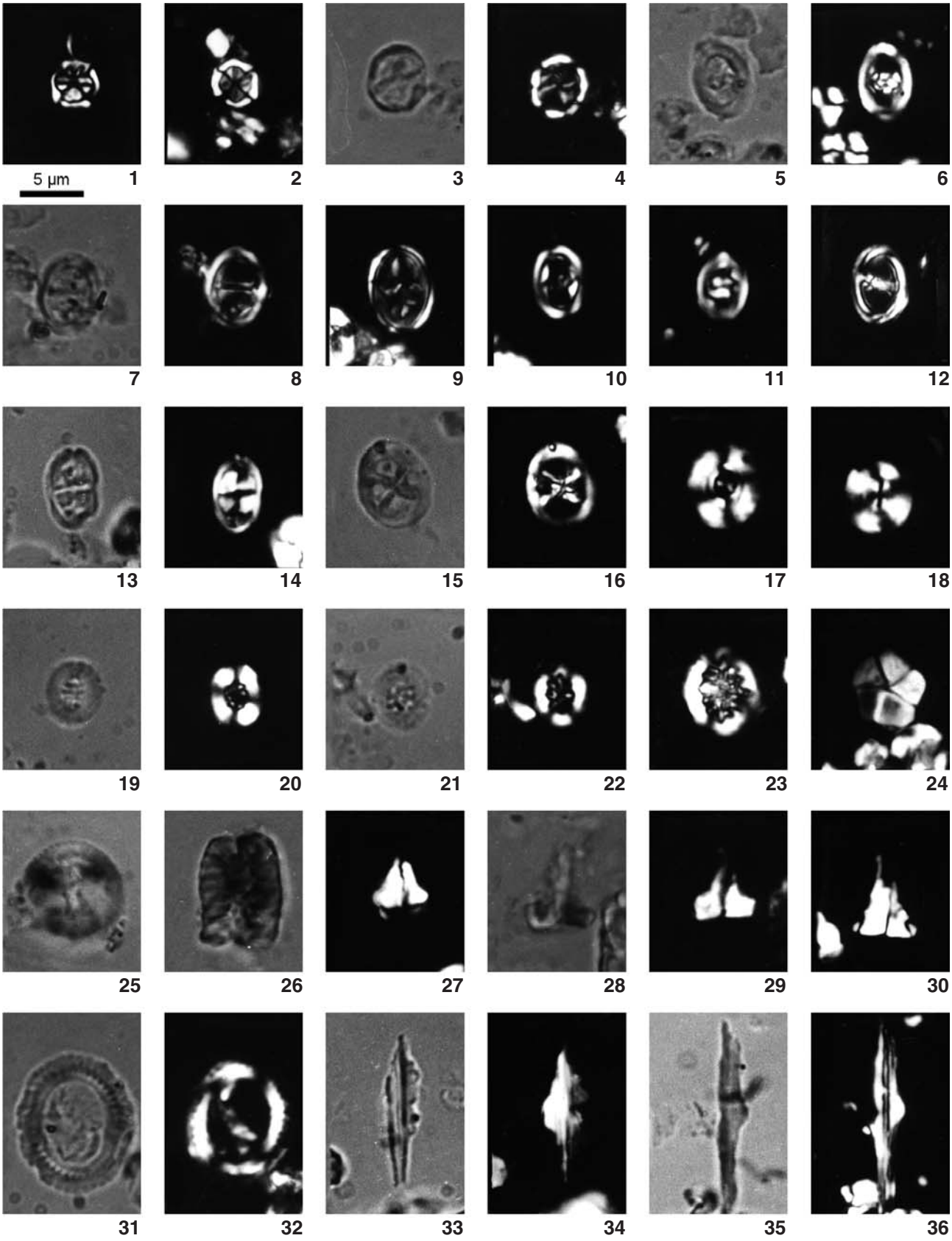
5 µm
1
2
3
4
5
6
7
8
9
10
11
12
13
14
15
16
17
18
19
20
21
22
23
24
25
26
27
28
29
30
31
32
33
34
35
36

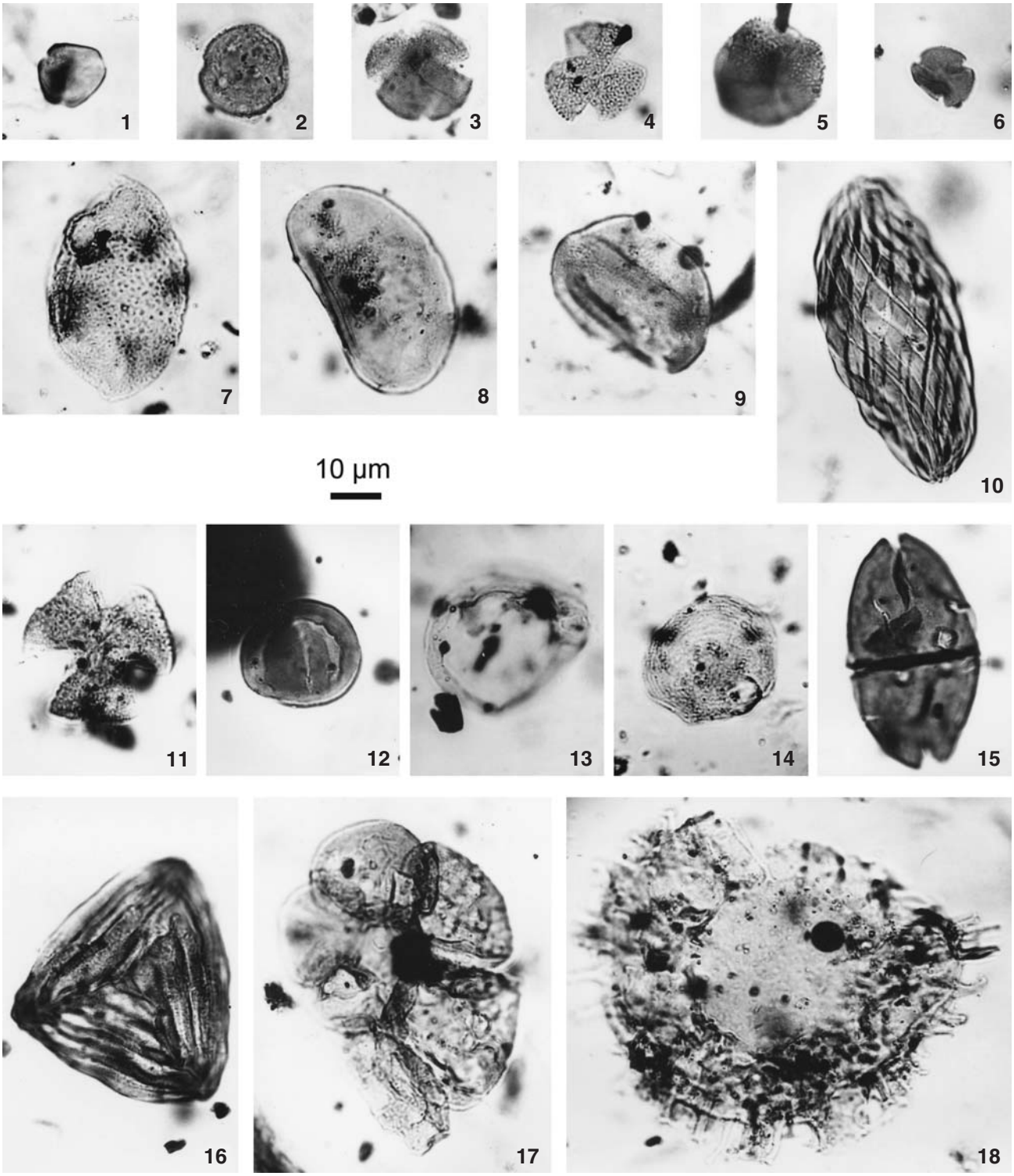
1
2
3
4
5
6
7
8
9
10
10 µm
11
12
13
14
15
16
17
18